A FIRST PRINCIPLE CALCULATION ON THE STRUCTURAL, MECHANICAL, ELECTRONIC AND OPTICAL PROPERTIES OF PbTe PEROVSKITE MATERIAL

BY

AKANDE FRIDAY ALABA

PSC2008336

DEPARTMENT OF PHYSICS

FACULTY OF PHYSICAL SCIENCES

UNIVERSITY OF BENIN

BENIN CITY

FEBRUARY, 2025

A FIRST PRINCIPLE CALCULATION ON THE STRUCTURAL, MECHANICAL, ELECTRONIC AND OPTICAL PROPERTIES OF PbTe PEROVSKITE MATERIAL

AKANDE FRIDAY ALABA

PSC2008336

SUBMITTED TO

DEPARTMENT OF PHYSICS,

FACULTY OF PHYSICAL SCIENCES,

UNIVERSITY OF BENIN, BENIN CITY, NIGERIA.

IN PARTIAL FULFILLMENT OF THE REQUIREMENTS FOR THE AWARD OF BACHELOR OF SCIENCE (B.Sc.) IN INDUSTRIAL PHYSICS

FEBRUARY, 2025

CERTIFICATION

This is to certify that this project work was carried out by **AKANDE FRIDAY ALABA** with Matriculation Number **PSC2008336**, of the Department of Physics, Faculty of Physical Sciences, University of Benin, Benin City, Edo State, Nigeria.

PROF B. E. IYORZOR	**Date**
(Project Supervisor)	
PROF. C.O AIGBOGUN	**Date**
(Head of Department)	
External Examiner	**Date**

DEDICATION

I dedicate this project to God Almighty my creator, my strong pillar, my source of inspiration, wisdom, knowledge and understanding. He has been the source of my strength throughout this project and on His wings only have I soared. I also dedicate it to my wonderful family members, whose love, support, and kindness have enabled me to finish this work.

CERTIFICATION OF DISSERTATION ON PLAGIARISM

We the undersigned attest and declare that the dissertation of **AKANDE FRIDAY ALABA** titled **' the first principle calculations on the Structural, mechanical, electronic, and optical properties of PbTe perovskite materia**l ' was carried out has successfully passed the anti-plagiarism test and doesn't violate any copyright.

_____ _____

PROF B. E. IYORZOR **Date**

(Project Supervisor)

_____ _____

PROF. C.O AIGBOGUN **Date**

(Head of Department)

ACKNOWLEDGEMENT

My sincere gratitude goes out to my supervisor, Prof. B.E. Iyorzor, for his helpful advice, ideas, and support in finishing this project. I want to express my gratitude to the Physics Department for providing the opportunity to complete the research successfully. I would especially like to thank my parents, Mr. Monday Akande and Mrs. Kehinde Akande, for their love and support of my academic endeavors. Furthermore, I would be remiss if I did not give credit to Mr. Benjamin, Mr. Moses Akande, Mrs. Rachael, and Mrs. Linda Oyeveshoso, whose concern and encouragement propelled me through my academic career. In conclusion, I would like to thank Doro, Elijah, Lizzy, Francis, and Nathan for their cooperation and friendship during this experience.

TABLE OF CONTENTS

ABSTRACT

Perovskite materials made of lead telluride (PbTe) have gained a lot of attention from researchers because of its potential uses in photovoltaics, optoelectronics, and thermoelectrics. They cannot, however, be fully utilized in device applications due to issues such as structural instability, mechanical constraints, electronic flaws, and suboptimal optical performance.

In order to solve these problems, we comprehensively examine the structural, mechanical, electronic, and optical characteristics of PbTe perovskite using first-principles density functional theory (DFT) computations. Through the analysis of elastic constants, and formation energies, our study unveils the basic stability criteria. The mechanical resilience of the material is assessed by evaluating its mechanical properties, such as bulk modulus, shear modulus, and Poisson's ratio.

Additionally, the nature of bandgap engineering and defect tolerance can be understood through the use of density of states and electronic band structure simulations. The dielectric function and absorption coefficient are examples of optical response functions that are calculated to maximize light-harvesting efficiency. Our findings point to potential strain engineering and doping techniques to improve PbTe's stability, electrical performance, and optical activity, hence increasing its suitability for use in next-generation energy and optoelectronic applications.

CHAPTER ONE

INTRODUCTION

1.1 What are Perovskite Material

Perovskite is a mineral composed of calcium titanium oxide, represented by the chemical formula $CaTiO_3$. The terms "perovskite" and "perovskite structure" are frequently used interchangeably, but there is a distinction. True perovskite (the mineral) consists of calcium, titanium, and oxygen in the composition $CaTiO_3$.

On the other hand, a perovskite structure refers to any material that follows the generic form ABX_3 and shares the same crystallographic structure as perovskite (the mineral). Perovskite is a mineral that features a specific structure where two cations, labeled as 'A' and 'B', have significantly different sizes, while 'X' serves as the anion that bonds to both. This mineral is commonly found in carbonate skarns at Magnet Cove, Arkansas, in altered limestone blocks from Mount Vesuvius, as well as in chlorite and talc schists in the Urals and Switzerland. Additionally, perovskite is present as an accessory mineral in alkaline and mafic igneous rocks.

1.1.1 Where do Perovskite Materials Come From

Perovskite is a mineral consisting of calcium titanate ($CaTiO_3$). The term "perovskite" refers to a group of compounds with the same crystal structure as $CaTiO_3$ ($XIIA_2+VIB_4+X_2-3$), known as the perovskite structure. This structure allows for the incorporation of various cations, enabling the creation of a wide range of engineered materials. Perovskite was first identified by Gustav Rose in 1839 in the Ural Mountains of Russia. He chose to name the mineral after the Russian mineralogist Lev Perovski (1792–1856).

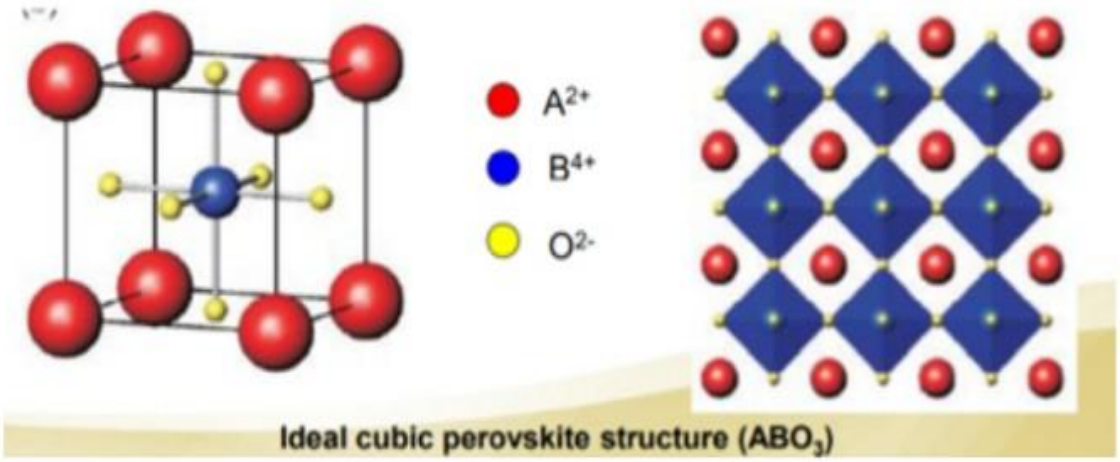

Fig.1.1. The ideal cubic perovskite structure (ABO_3) (Zhou et al., 2018)

1.1.2 How are Perovskite Materials Made

Perovskite structures are typically represented by the formula ABX_3, and any crystal structure following this pattern is identified as a perovskite. True perovskite material is produced as $CaTiO_3$ using oxygen, titanium, and calcium. However, the term perovskite is also used to describe a category of ceramic oxides with the formula ABX. These compounds are categorized as alkaline metal halide perovskites, inorganic oxide perovskites, and organic metal halide perovskites. Bridgmanite, the most prevalent mineral in Earth's mantle, is a silicate represented by the formula (Mg, Fe) SiO_3. It exhibits a perovskite structure at high pressures. The SiO_{44}− tetrahedral units in silica-rich minerals become unstable as pressure increases in comparison to SiO_{68}− octahedral units. The second most common element, potentially (Mg, Fe) oxide-structured periclase, adopts a rock salt structure under the temperature and pressure conditions found in the lower mantle. Certain criteria must be met for the formation of a perovskite structure, including the total valences of A and B cations being three times greater than those of the X anion to maintain charge balance. Moreover, the perovskite framework is limited to specific ion pairings due to size constraints between ions to maintain the anion-corner-sharing

arrangement. This relationship in ionic sizes is quantified by the Goldschmidt tolerance factor τ, which is associated with the ionic rardii r_A, r_B, and r_X .

$$\tau = \frac{r_A + r_X}{\sqrt{2}(r_B + r_X)} \qquad (1.1)$$

The value of τ serves as a practical indicator for anticipating the various forms of ABX_3 structures. A τ value between 0.9 and 1 indicates the formation of a flawless cubic perovskite structure. In contrast, a τ value falling between 0.8 and 0.9 suggests a preference for a distorted perovskite structure characterized by tilted octahedra. When τ is less than 0.8 or greater than 1, the structure deviates from the perovskite arrangement.

1.1.3 Perovskite in Solar Technology

The field of solar technology has witnessed significant progress in recent times, with experts in the renewable energy sector constantly exploring innovative methods to provide sustainable power for the planet. One cutting-edge technology that is leading the way in the future of solar energy is perovskite solar cells. This raises questions about what are they,how do they work,what are their advantages and disadvantages and what impact do they offer to the solar energy sector. We will delve into all of the topics mentioned above in this comprehensive guide.

In this guide, we will explore the following:

a) What are perovskite solar cells
b) How do perovskite solar cells work
c) Advantages of perovskite solar cells
d) Disadvantages of perovskite solar cells
e) Perovskite solar panels pioneering the future of solar energy

a) What are Perovskite Solar Cells

A perovskite solar cell is a type of thin film photovoltaic device that uses perovskites to absorb sunlight and generate electrical energy. These perovskites possess key properties that make them well-suited for this purpose. When combined with specific inorganic and organic materials, perovskites can be converted into a semiconductor, serving as the ideal base for the development of highly efficient solar cells. Perovskite-based solar cells serve as the fundamental components for constructing solar panels. The composition of perovskite can be conveniently produced, positioning it as a leading contender in the advancement of solar power. Its economical nature and high performance are anticipated to have a significant impact on the development of next-generation electric vehicle batteries, lasers, sensors, and various other technologies.

The inaugural perovskite solar cell was pioneered by Tsutomu Miyasaka, a Japanese researcher, in the year 2009. In the early stages of testing, the technology exhibited a modest efficiency of 3%. However, significant advancements have been achieved since then, leading to perovskite solar panels now consistently achieving efficiencies exceeding 25%. Silicon, which is the semiconductor material present in 95% of the solar cells used in the production of current rooftop solar panels.

b) How do Perovskite Solar Cells Work

Perovskite solar cells consist of multiple layers and function based on the photovoltaic effect, which involves the generation of electric currents in a photovoltaic cell when exposed to sunlight – similar to conventional solar panels. When sunlight interacts with the perovskite absorber layer, electrons are released, forming electron-hole pairs. These electrons move towards the hole transport layer (HTL) and then to the conductor, which powers the connected load, leading to the generation of an electric current. After generating an electric current by passing through the load, electrons are gathered by the electron transport layer (ETL) in the perovskite solar panel, preventing any reverse flow of holes. Energy losses may occur during the perovskite solar power generation process, primarily due to surface recombination. In this phenomenon, released electrons combine with holes instead of contributing to the electric current flow. The

configuration of layers in a perovskite solar cell may differ, but it generally resembles that of a dye-sensitized solar cell (DSSC). The main distinction lies in the fact that, in a perovskite solar cell, a layer of perovskite material serves as the light-absorbing medium instead of a dye attached to a semiconductor surface. Perovskite solar cells differ from DSSCs by eliminating the requirement for a thick porous TiO_2 layer to aid in hole-electron pair separation. The unique structure of perovskite allows charges to efficiently move apart. Hole-transport materials, organic in nature, are frequently employed to transport holes away from the perovskite solar cells. These materials create a thin film on top of the perovskite layer, enabling the cell to transition into a solid state, eliminating the use of liquid electrolytes in DSSCs, which are susceptible to leaks. This new design enhances the efficiency and durability of perovskite solar cells, making them a highly regarded advancement in the progression of solar energy technology. Moreover, they are expected to be utilized in the most important sustainable energy initiatives in the foreseeable future.

c) Advantages of Perovskite Solar Cell Materials

The following are the benefits of perovskite solar cell:

1. Perovskite material offers direct optical band gap of around 1.5eV.
2. Perovskite material offers long diffusion length and long minority carrier lifetimes.
3. It has broad absorption range from visible to near infrared spectrum (800 nm) and high absorption coefficient (105 cm^{-1}).
4. Perovskite cells deliver efficiencies of more than 22 percent.
5. Perovskite material such as methylammonium lead halides are far inexpensive and simple to manufacture.
6. It has high dielectric constant, fast charge separation process, long transport distance of electrons and holes and long carrier separation lifetime.
7. This low cost material helps in converting windows of buildings, top of cars and walls to achieve solar power generation.

8. Perovskite uses less material in order to absorb same amount of light compare to silicon. Hence it is cheaper than silicon.

d) Disadvantages of Perovskite Solar Cell Materials

The following are the drawbacks of perovskite solar cell:

1. Degradation issue of methyl ammonium lead iodide Perovskite need to be studied.
2. Main issues in perovskite solar cells are film quality and thickness.
3. The perovskite material will break down quickly due to exposure of heat, moisture, snow etc.
4. The material is toxic in nature.

e) Perovskite Solar Panels Pioneering the Future of Solar Energy

Perovskite solar panels have gained considerable interest in recent years for their exceptional efficiency improvements, attracting the attention of researchers, industry professionals, and environmental advocates. A report by The Independent highlighted the significant efficiency advancements demonstrated by these solar panels in the UK, surpassing levels previously believed to be unachievable by conventional photovoltaic technologies. This innovative approach to utilizing solar power has the potential to revolutionize the renewable energy sector. According to the research findings, Qcells, a PV manufacturer based in South Korea, is planning to allocate $100 million towards the development of perovskite solar cells. They are optimistic about the potential of this solar technology to achieve efficiency improvements ranging from 50% to 75% when compared to conventional solar panels. In a recent development reported by TechXplore, researchers at Northwestern University have successfully increased the efficiency of inverted perovskite solar cells to over 25%. The innovative inversion design has demonstrated significant enhancements in the performance of these solar cells, leading to further advancements in efficiency levels. The ongoing effort to improve efficiency highlights the dedication of scientists and engineers in harnessing the complete capabilities of perovskite technology. Furthermore, in

May 2023, Oxford PV set a new world record for efficiency in a commercial-sized tandem solar cell, achieving efficiencies exceeding 28%. Tandem solar cells combine multiple solar cells in a stack to increase energy conversion from sunlight. This notable achievement brings perovskite solar panels closer to being economically feasible. Additionally, combining perovskite and silicon in tandem solar cells has expanded the possibilities for increased efficiency. According to PV Magazine, this tandem method has shown a practical efficiency potential of 39.5%. The significant progress made by researchers at the German Fraunhofer Institute for Solar Energy Systems (Fraunhofer ISE) represents a major breakthrough in the field of solar energy generation. This achievement paves the way for reaching new heights of efficiency in harnessing solar power.

1.1.4 USES OF PEROVSKITE MATERIALS

The following are some of the uses:

1. **Thermoelectric Devices:** Conversion of waste heat into electrical energy
2. **Battery Electrodes:** High ionic conductivity for lithium-ion batteries and other energy storage devices
3. **Catalysts: Chemical** reactions, including water splitting for hydrogen production
4. **Lasers:** Low threshold energy for various optical applications
5. **Photodetectors**: High sensitivity for imaging and sensing
6. **Solar Cells:** High efficiency and low-cost production
7. **For Light-Emitting Diodes (LEDs).**

The elements listed in Figure 1.2 below of the periodic table are typically located in either the A or B site cationic positions within the perovskite structure. With the exception of gases or liquids under standard conditions, most elements have the potential to occupy these specific positions within the structure.

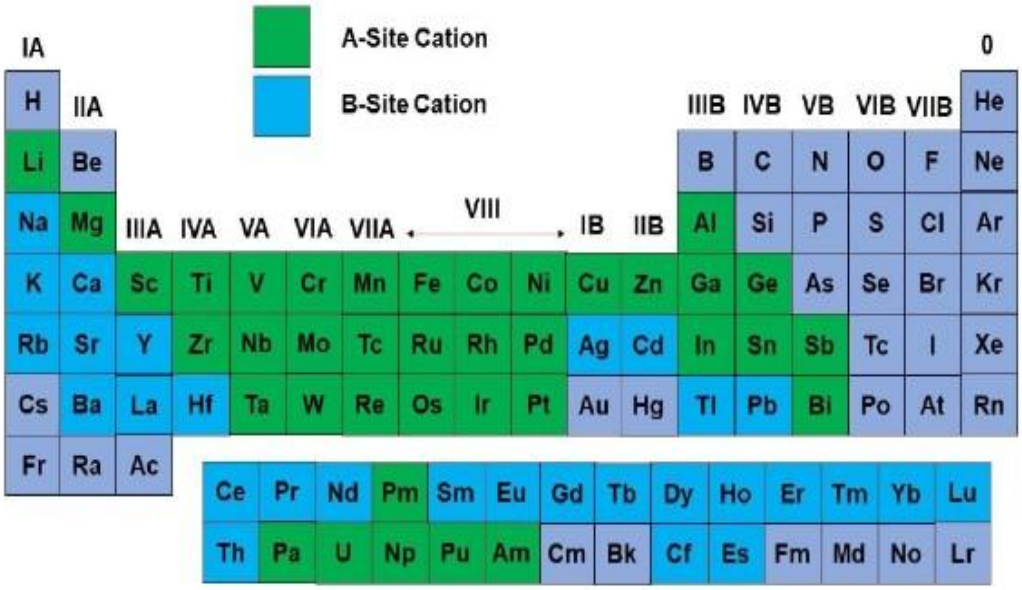

Fig.1.2. Periodic table showing the elements that occupy A or B site cationic positions in the perovskite structure.

Figure 1.3. Illustrates the arrangement of the perovskite lattice structure. In structural science and crystallography, perovskites can be depicted in various forms. A straightforward representation of a perovskite structure involves a central cube with a large atomic or molecular cation (positively charged) of type A. The corners of the cube are filled with ions of type B (also positively charged cations), while the faces of the cube are occupied by the anion X with a negative charge.

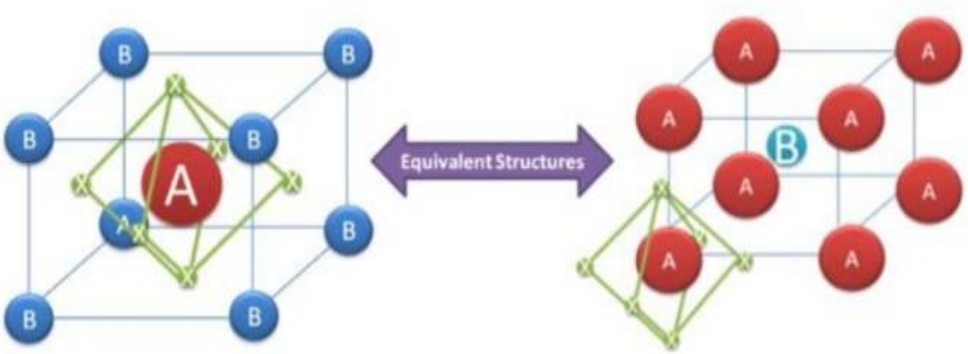

Fig.1.3. Two equivalent structures of perovskite structures with left-hand side is drawn with B site ion at <0,0,0> and the right-hand diagram with A site ions at <0,0,0> position .

Numerous oxide compounds are recognized as part of several perovskite-based homologous series, such as the $A_{n+1}B_nO_{3n+1}$ Ruddlesden-Popper series, $A_nB_nO_{3n+1}$ Dion-Jacobson series, $Bi_2A_{n-1}B_nO_{3n+3}$ Aurivillius series, and some others. The perovskite structures are found in various forms, including ABO_3-perovskite (e.g. $BaTiO_3$, $CaTiO_3$), A_2BO_4-Layered perovskite (e.g. Sr_2RuO_4, K_2NiF_4), A_2 BB'O_6-Double perovskite (e.g. Ba_2TiRuO_6), and $A_2A'B_2B'O_9$-Triple perovskite (e.g. $La_2SrCo_2FeO_9$). Many perovskite-type oxides have been extensively researched for their unique properties such as superconductivity, insulator-metal transition, ionic conduction characteristics, dielectric properties, optoelectronic properties, and ferroelectricity. Perovskite is a widely studied structure in solid-state chemistry, capable of accommodating a variety of metal ions from the periodic table along with different anions. In recent years, there has been significant research conducted on perovskite solids, particularly ABO_3 compounds. These materials are increasingly significant in various fields such as electrical ceramics, refractories, geophysics, material science, astrophysics, particle accelerators, fission-fusion reactors, heterogeneous catalysis, environmental applications, and more. Perovskite structured oxides have the ability to accommodate significant substitutions in either one or both cationic sites (referred to as A and B sites), without altering their original crystal structures. This characteristic allows for chemical customization of the materials by partially replacing the cationic site(s) with

foreign metal ions, thereby altering their structural, microstructural, electrical, and magnetic properties. Perovskite-type oxides and similar compounds have been utilized in various applications in the fields of physics and chemistry. The characteristics and uses of perovskites are influenced by factors such as crystal structure, lattice defects, exposed lattice planes, surface morphology, particle size, specific surface area, and porous texture. The cubic perovskite is considered the most ideal form. These materials hold great promise for a range of device applications because of their uncomplicated crystal structures and distinctive ferroelectric and dielectric properties.

Perovskite systems have the ability to form crystals in diverse compositions, including various combinations of cations such as $A^{+}B^{5+}$, $A^{2+}B^{4+}$, $A^{3+}B^{3+}$, as well as different defect compositions within ABX_3 systems. This concept is illustrated in the accompanying flow diagram (Fig.1.4.) with examples provided.

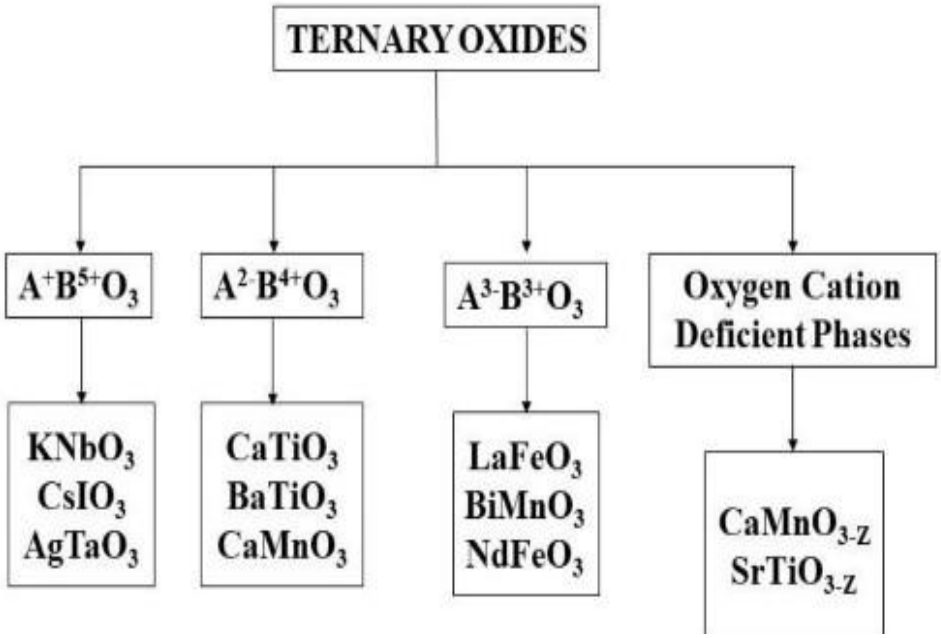

Fig.1.4. Flow diagram of the generation of a variety of compositions in ABX3 systems

1.2 PROPERTIES OF PEROVSKITE

Perovskite materials possess a large range of properties as a result of their distinctive chemical composition. These properties include non-stoichiometry of anions and/or cations, a mixed

valence electronic structure, cation configuration distortion, and mixed valence characteristics (Kim et al., 2005). Some of these properties are given as follows:

1.2.1 Dielectric Properties

Dielectric materials are materials that can retain electro-static fields for an extended period (Niu et al., 2015). They exhibit high resistance to electric current flow when subjected to direct current voltage, and their electrical properties differ significantly from conductive materials. These materials are often used in capacitors to enhance their efficiency, giving rise to the term dielectric (Xiao et al., 2011).

High dielectric permittivity or ferroelectric materials play a significant role as electroceramics in the engineering and electronics sector. The concept of ferroelectricity is commonly explained through a soft-mode model (Hoefler et al.,2017)

1.2.2 Optical Properties

Perovskite have emerged as a unique category of materials known for their outstanding optical and photoluminescence characteristics. A study conducted by Ohta and Hiramatsu in 2018 examined the optical properties of single domain crystals of $BaTiO_3$ across different temperatures. The research revealed that the refractive index of the crystal remained relatively constant at 2.4 between 20° to 90 °C, but increased to 2.46 at 120 °C (Zhang et al.,2017). Moreover, the study found that a single crystal of $BaTiO_3$, measuring 0.25 mm in thickness, exhibited transmission capabilities ranging from 0.5 μ to 6 μ. The optical coefficient of strontium titanate single crystals was obtained across a range of wavelengths from 0.20 μ to 17 μ (Xin et al., 2019).

Potassium tantalate niobate (KTN) is a type of perovskite oxide known for its significant room temperature electro-optic effect and wide-angle fast optical beam scanning capabilities. This characteristic makes it valuable not only for optical communications but also for a variety of other products utilizing optical beams, including laser applications (Wang et al., 2008) while environmental friendly photoluminescence (PL) materials like $BaZrO_3$ emit light in the visible

range, offering potential uses in scintillators, solid state lightning, field emission displays, green photocatalyst and plasma displays (Sayyadi-Shahraki et al., 2017).

1.2.3 Ferroelectricity

Ferroelectricity is the occurrence of spontaneous electric polarization in certain materials when subjected to an external electric field (Retot et al., 2008; Cross, 2011).

The ferroelectric materials have dielectric constant twice as large in magnitude than those in ordinary dielectric. $BaTiO_3$ is a widely recognized ferroelectric material with a high relative dielectric constant. At room temperature, its crystal structure does not have a permanent polarization in the absence of an external field, despite the alignment of dipoles in neighboring unit cells (Xu, 2011). The ferroelectric property finds various applications including ultrasound imaging devices, fire sensors, infrared cameras, vibration sensors, tunable capacitors, memory devices, RAM, and RFID cards. It is also utilized in input devices for ultrasound imaging and sensors, as well as in capacitors and memory devices (Raghavan, 2015).

1.2.4. Superconductivity

Superconductivity is a phenomenon where certain materials, when cooled to a very low temperature, show no electrical resistance(zero) and can expel magnetic fields (Kittel, 2005).

The perovskite structure type with oxide compounds serves as a strong structural foundation that enables superconductivity. Perovskites containing copper exhibit high-temperature superconducting properties. One of the initial instances of superconducting perovskites is the La-Ba-Cu-O perovskite, with numerous others discovered (Mourachkine, 2004). Perovskite oxides have now surpassed Intermetallic compounds in serving as the primary source for numerous superconducting materials, including cesium tungsten bronzes and alkali metals like sodium, potassium, and rubidium (Cava, 2008).

1.2.5 Piezoelectricity

Piezoelectricity refers to the phenomenon where certain materials are able to generate an electric charge when subjected to mechanical stress (Wang et al. 2004). Hence, when specific crystals

undergo mechanical stress, they exhibit polarization that is directly proportional to the amount of strain applied (Wang et al., 2006). However, their behavior was altered when subjected to an electric field, a phenomenon referred to as the inverse piezoelectric effect (Brockmann, 2009).

Piezoelectric ceramics with the perovskite crystal structure, characterized by the general formula $A^{2}+B^{4}+O_{2}-3$, are among the synthetic materials exhibiting piezoelectric properties (Aksel et al., 2011). In addition to these synthetic materials, there are naturally occurring piezoelectric materials such as quartz, cane sugar, collagen, topaz, rochelle salt, and tendon.

1.2.6 Multiferroicity

Multiferroics are a unique group of materials that exhibit simultaneous ferroelectric, ferromagnetic, and ferroelastic properties. Their distinct feature lies in their capability to utilize both their magnetization and polarization states concurrently. This characteristic makes them highly suitable for use in memory devices and sensors (Spaldin et al., 2010, Ramesh and Spaldin, 2007). Numerous multiferroics are comprised of transition metal oxides with a perovskite crystal structure, such as rare-earth manganite and ferrites (Wang et al., 2010). These materials exhibit multiferroicity even when maintained at room temperature (Kézsmárki et al., 2011). Bismuth ferrite, characterized by a rhombohedrally distorted perovskite structure (compounds with multiferroic properties), displays both anti-ferromagnetic and ferroelectric order over a wide temperature range that extends well beyond room temperature (Singh et al., 2011).This unique combination of properties in perovskite-based multiferroics offers great potential for applications in various fields,such as spintronics devices and designing novel microelectronic (Bai et al., 2005).

1.2.7 Catalytic activity

Perovskites exhibit remarkable catalytic activity and excellent chemical stability, making them suitable for catalyzing various reactions. They are often referred to as oxidation or oxygen-activated catalysts and serve as a representation of active sites (Roni, 2018).

1.2.8 Colossal Magneto Resistance (CMR)

Colossal magneto-resistance (CMR) is a unique characteristic found in certain materials, primarily manganese-based perovskite oxides, which enables them to alter their electrical resistance when exposed to a magnetic field (Lu et al., 2004). This discovery of CMR has had an impact on the perovskite manganite $RE_{1-x}AE_xMnO_3$, which is doped with divalent alkaline-earth ions represented by AE (such as Ca, Sr, Ba) and trivalent rare-earth ions represented by RE (such as La, Pr, Sm, etc.) (Garg et al., 2009).

1.3 Application of Perovskite

Perovskite materials have a wide range of applications due to its stable structure, large number of compounds, variety of properties.The application of perovskite-based include;Gas sensor, glucose sensor, neurotransmitters sensor, solid oxide fuel cells, catalyst, solar cells etc (Deka et al., 2014).

1.3.1 Gas Sensors

Gas devices must meet specific requirements in order to be considered suitable for use as fuel sources. These requirements include hydrothermal stability, compatibility with the gases they are intended to work with, appropriate electronic configuration, resistance to contamination, and the ability to integrate with current technologies (Christen and Eres, 2008).

Perovskite oxides such as $LaFeO_3$ and $SrTiO_3$ are commonly utilized as gas sensors due to their semiconductor-like properties. These materials are favored for gas sensing applications because of their optimal band gap, stable thermal characteristics, and the disparity in size between the cations found at the A- and B- sites. Various perovskite materials containing cobaltates, titanates, and ferrites have been employed as gas sensors to detect gases like CO, NO_2, methanol, ethanol, and hydrocarbons (Taylor et al., 2019).

1.3.2. Glucose Sensor

Analyzing H_2O_2 and glucose is crucial in various industries like food, pharmaceuticals, and healthcare settings. H_2O_2 serves as an oxidizing agent in numerous sectors, while glucose plays a

vital role as a fundamental metabolite in living organisms. It is essential for monitoring diabetes mellitus and overall health. Having highly sensitive biosensors is crucial for detecting both H_2O_2 and glucose accurately (Ottochian et al. in 2014).

Various types of enzymatic glucose sensors exist, however, they lack stability due to their basic nature and are easily influenced by external factors like toxic substances, temperature, and humidity. Therefore, it is necessary to explore non-enzymatic glucose sensors that are stable, sensitive, simple, and selective, such as inorganic perovskite oxides (Jia et al., 2015).

The sensor exhibits excellent electrocatalytic performance for the oxidation of glucose and H_2O_2 in an alkaline solution, attributed to the presence of a large number of active sites in the modifier.

1.3.3 Neurotransmitters Sensor

Dopamine (DA) is a crucial catecholamine neurotransmitter in the mammalian central nervous system. The lack of this neurotransmitter is linked to Parkinson's disease, making its detection vital. However, a major challenge in detecting DA arises from the interference of ascorbic acid (AA) and uric acid (UA) (Jia et al., 2015). Thus, it is very important to develop a highly sensitive and selective detector for DA even in the presence of high levels of AA and UA**.**

Following the modification of the electrode with $SrPdO_3$ (CpE/$SrPdO_3$), it exhibited excellent electrochemical properties as a dopamine (DA) sensor in biological fluids, showing remarkable long-term stability and a low detection limit even in the presence of high concentrations of ascorbic acid (AA) and uric acid (UA). Moreover, it demonstrated the ability to selectively detect DA in human urine samples with high selectivity, recovery, precision, accuracy, and a low detection limit (Zhang et al., 2013).

1.3.4 Solid Oxide Fuel Cells

Fuel cells are utilized as alternatives to combustion engines because of their ability to decrease environmental pollution. They utilize a particular chemical compound as a fuel source that is converted into electrical energy similar to a battery. Fuel cells are favored for their efficiency, widespread availability, lack of noise pollution, low emissions, and their role in the future

hydrogen fuel economy. There are various types of fuel cells, with solid oxide fuel cells being the most commonly used examples (El-Ads et al., 2015).

Perovskites are chosen as a key component in Solid Oxide Fuel Cells (SOFC) due to their diverse electrical conductive properties. They demonstrate high electrical conductivity similar to metals, along with excellent mixed ionic and electronic conductivity. (Wang et al., 2012; Atta et al., 2013).

1.3.5 Catalyst

Perovskite oxides are commonly utilized as catalysts in modern chemical production due to their favorable solid-state, surface, and morphological characteristics (Thirumalairajan et al., 2013). Numerous perovskite oxides have demonstrated impressive catalytic performance in various reactions such as hydrogen evolution, reduction reactions, and oxygen evolution (Lianghao et al., 2015).

1.3.6 Solar Cells

Solar energy is considered a sustainable alternative to fossil fuels, as it harnesses the power of solar radiation to generate electricity through photovoltaic solar cells made of silicon. This renewable energy source offers a wide range of applications and benefits. The primary drawback of silicon-based solar cells is the high cost of the electricity they generate, highlighting the necessity for the development of more cost-effective solar cell technologies (Wang et al., 2012; Li et al., 2016).

Solar cells made from a combination of organic and inorganic solid-state methyl ammonium lead halide hybrid perovskite have gained popularity due to their cost-effectiveness compared to traditional silicon solar cells, with a reduction of up to 20%. Additionally, the raw materials required for these perovskite solar cells are more readily available. Perovskite has shown to possess important properties necessary for photovoltaic applications, including a suitable band gap, excellent stability, long hole-electron diffusion length, high absorption coefficient, high

carrier mobility and transport, low processing temperature, charge carriers with small effective mass, and simplified processing steps. (Jin et al., 2013; Bao et al., 2015).

1.4 Aim and Objectives

AIM

The aim of this research is to investigate the ground state energy and physical characteristics of PbTe.

OBJECTIVES

The objectives of this research are to;

1. Calculate the mechanical properties of the compound (elastic constant, shear modulus, Young's modulus).
2. Calculate the structural properties (lattice constant, bulk constant, modulus, pressure derivatives).
3. Calculate the electronic properties of the compound (band structure, DOS, material type).
4. Calculate the optical properties of the compound (dielectric function, refractive index, absorption coefficient, and energy loss function).

CHAPTER TWO

LITERATURE REVIEW

2.1 PbTe Perovskite compound

Lead telluride (PbTe) is an important semiconducting semiconductor, best known for its thermoelectric properties. It belongs to the perovskite family of materials, which are well-known for their diverse electronic, optical, and mechanical properties. PbTe has undergone substantial research due to its potential applications in thermoelectric energy conversion, infrared sensors, and photovoltaics. This literature review examines the structural, mechanical, electronic, and optical properties of PbTe perovskite materials, and concludes with a discussion of the future prospects for PbTe-based materials.

2.1.1 Structural Properties:

PbTe crystallizes in a face-centered cubic (FCC) structure, with each Pb and Te atom creating a rock salt (NaCl) lattice. At room temperature, PbTe has excellent structural stability, making it a suitable option for a wide range of applications. The lattice constant, around 6.46 Å, influences the material's electrical properties and stability in various settings. Under pressure, PbTe undergoes phase transitions, such as from cubic to orthorhombic, which affects its thermoelectric properties.

PbTe has a moderate bulk modulus, indicating that it is generally resistant to volumetric changes caused by applied stress. This mechanical robustness is critical in thermoelectric applications that subject materials to heat and mechanical pressures. Computational studies using density functional theory (DFT) have revealed information about its elastic moduli and phonon dispersion relationships. These findings imply that the material's stability is impacted by its phonon scattering properties, which are critical for thermoelectric performance.

2.1.2 Mechanical Properties:

PbTe has moderate mechanical stiffness, and elastic moduli indicate that it is somewhat ductile under certain stress levels. According to first-principles calculations, PbTe's mechanical characteristics are very anisotropic. This means that its stress response varies depending on the

crystallographic orientation, which is useful for applications that require material flexibility, such as flexible thermoelectrics or optoelectronics. Doping and nanostructuring can improve the material's mechanical strength, resulting in better performance in practical applications.

2.1.3 Electronic Properties:

PbTe is a direct bandgap semiconductor with a bandgap of around 0.3-0.6 eV at ambient temperature. Its electronic structure is distinguished by significant spin-orbit coupling (SOC), which affects both conductivity and band structure. Without SOC, PbTe has a considerably broad bandgap at the Γ point. However, incorporating SOC reduces the bandgap and causes band inversion at the X point in the Brillouin zone, a characteristic of topological crystalline insulator (TCI) behavior. This characteristic makes PbTe a promising candidate for quantum computing and spintronics applications.

In PbTe, the electronic band structure is mainly influenced by Pb-p and Te-p orbitals. The conduction band is mostly Pb-pz, while the valence band is primarily Te-px,y states. By doping PbTe with elements like Na or Sb, the carrier concentration can be enhanced, leading to improved electrical conductivity without majorly affecting the Seebeck coefficient. Computational techniques, such as hybrid functional calculations, suggest that PbTe can be adjusted further to achieve specific electronic properties suitable for thermoelectric and optoelectronic uses.

2.1.4 Optical Properties:

The optical characteristics of PbTe play a significant role in its applications in photovoltaic technology and infrared photodetectors. PbTe demonstrates high absorption rates in the infrared spectrum, making it well-suited for use in infrared sensors. Its absorption capacity notably rises within the 1.0 to 5.0 eV range, with peak values occurring around 3.5 eV, aligning with its electronic transitions through the bandgap. Research utilizing Density Functional Theory (DFT) and hybrid functional techniques has shown that the optical conductivity and dielectric function

of PbTe display notable changes in response to doping, as well as external influences such as pressure and strain.

The refractive index of PbTe is approximately 2.67, making it ideal for enhancing photon absorption in photovoltaic technology. The intricate dielectric properties of PbTe in the infrared and visible spectrums make it a suitable choice for optoelectronic devices, enabling effective light absorption and separation of charges crucial for energy conversion processes.

2.1.5 Thermoelectric Properties:

PbTe has been widely researched as a thermoelectric material for its superior performance within the temperature range of 500-800 K. The enhancement of its figure of merit, ZT, has been achieved through various methods such as doping, nanostructuring, and creating composites. The introduction of alkali metals, alkaline earth metals, and rare earth elements through doping has notably enhanced both the electrical conductivity and thermoelectric efficiency of PbTe. Utilizing nanostructuring methods, such as incorporating quantum dots or nanowires, has significantly improved the thermoelectric characteristics of the material by decreasing heat conductivity through phonon scattering while preserving a high level of electrical conductivity**.**

The thermoelectric efficiency of PbTe is greatly influenced by its carrier concentration, which can be adjusted by manipulating its doping levels. Moreover, PbTe can be alloyed with other substances like PbSe or SnTe to create materials with improved thermoelectric properties. This adaptability makes PbTe a promising choice for applications in energy generation, specifically in converting waste heat into valuable electrical power.

2.2 Future Prospects:

The future of PbTe lies in several promising research avenues:

(1) Lead-Free Alternatives: Extensive research has been conducted on lead-free alternatives, such as SnTe, in response to environmental concerns regarding lead toxicity. These alternatives, like SnTe, seek to maintain the desirable properties of PbTe while being more eco-friendly. The

primary goal is to minimize environmental impact without compromising the high performance required in thermoelectrics and optoelectronics (Liu et al., 2023).

(2) Enhanced Thermoelectric Performance: Current research is centered on enhancing the thermoelectric figure of merit (ZT) of PbTe through increased electrical conductivity and decreased thermal conductivity. Nanostructuring and doping are crucial methods for enhancing thermoelectric efficiency. Additionally, the incorporation of high-performance thermoelectric composites could boost the material's potential in energy harvesting applications (Li et al., 2023).

(3) Quantum and Topological Electronics: The identification of PbTe as a topological crystalline insulator (TCI) presents promising prospects in the fields of quantum computing and spintronics. With its unique characteristic of hosting topologically safeguarded surface states, alongside its insulating properties in the bulk, PbTe emerges as a prime contender for the advancement of innovative quantum electronics and quantum computer technologies (Zhang et al., 2022).

(4) Flexible Electronics: Experts are currently studying the characteristics of PbTe for potential applications in flexible electronics, including wearable thermoelectric devices and solar cells. The research is centered on enhancing PbTe's mechanical flexibility and optical transparency while maintaining its exceptional electronic properties (Fang et al., 2021).

CHAPTER THREE

METHODOLOGY

3.1 Density Functional Theory (DFT)

Density functional theory (DFT) is a computational method based on quantum mechanics that is widely employed in physics, chemistry, and materials science to analyze the electronic or nuclear structure, primarily the ground state, of complex systems such as atoms, molecules, and condensed phases. By utilizing functionals, which are mathematical functions that take another function as input and produce a single real number as output, DFT allows for the determination of various properties of a system with multiple electrons. In the context of DFT, these functionals are dependent on the spatial distribution of electron density. Density Functional Theory (DFT) is widely recognized as one of the most versatile and commonly used techniques in the fields of condensed-matter physics, computational physics, and computational chemistry. DFT has been widely utilized for computations in the field of solid-state physics since the 1970s. It is now commonly used for determining properties such as the binding energy of molecules in chemistry and the band structure of solids in physics (Klause Capella, 2006). Quantum mechanics involves the wave function of a system, which holds comprehensive data about the system based on electronic coordinates. The Schrodinger equation is utilized to determine the wave function of a lone electron in motion within a potential, excluding considerations of relativity.

In computational material science, ab initio DFT calculations allow for the prediction of material behavior using quantum mechanical principles, without the need for additional parameters such as fundamental material properties. Modern DFT techniques utilize a potential that influences a system's electrons to analyze its electronic structure. The overall potential, V, consists of external potentials, V_{ext}, determined by the system's structure and elemental makeup, and the effective potential, Veff, which accounts for interactions between electrons.

Density functional theory (DFT) is based on the concept that the characteristics of the lowest energy state(ground state) of a system with many electrons can be derived from its electron

distribution, rather than relying on wave functions as in traditional approaches. Through the use of the Hohenberg-Kohn theorems, DFT establishes a direct correlation between the electron density and the system's energy. In order to simplify the solution of the Schrödinger equation for systems with multiple particles, a more tractable approach is employed. This equation is known for its complexity when applied to systems with multiple interacting particles. To better understand this method, let us examine the following approaches :

3.1.1 Hohenberg-Kohn Theorem 1

The external potential energy V_{ext} or V(r) is determined by the ground state density n(r) up to a simple constant term.

So what the Hohenberg-Kohn theorem suggests may not sound trivial. The Schrödinger equation describes how we can obtain the wavefunction from a given potential. Once the wavefunction has been solved (which may be challenging), we may calculate the density and other parameters. According to the Hohenberg-Kohn theorem, the inverse is also true. The potential of a particular density can be determined uniquely. For non-degenerate ground states, no two Hamiltonians may have the same ground-state electron density. It is feasible to define ground-state energy in terms of electronic density.

3.1.2 Hohenberg-Kohn Theorem 2

The total energy of the system reaches its lowest value E(n) when the electron density n(r) corresponds to the true ground-state density, out of all potential electron densities.

The lowest (ground) energy state can be determined by minimizing E(n) rather than solving for the wavefunction of multiple electrons. It is important to understand that HK theorems do not provide information on how the energy changes with the electron density. In practice, the exact E(n) is generally unknown except for specific scenarios, leading to the utilization of approximate functionals. The fundamental principle of the Hohenberg-Kohn theorem states that the ground-state wave function, which is not degenerate, is exclusively determined by the ground-state density :

$$\psi_0(r_1, r_2, \ldots, r_N) = \psi[n_0(r)] \qquad (3.1)$$

3.1.3 Kohn-Sham hypothesis (KS)

The theorems given by Hohenberg-Kohn are exact; however not very useful in real calculations.

The equation given by Kohn-Sham turned DFT into an applied tool where in the presence of an external potential Vext(r), any set of N interacting electrons can be represented by an equivalent system of N non-interacting electrons with identical density. These non-interacting electrons are influenced by a distinct external potential (pertaining to single particles).

$$\left(-\left(\frac{\hbar^2}{2m}\right)\nabla^2 + v_{eff}(r)\right)\varphi_i = \varepsilon_i\varphi_i(r) \qquad (3.2)$$

$$v_s(r) = v_{ext}(\mathrm{r}) + \mathrm{e}^2 \int \mathrm{d}^3\mathrm{r}' \frac{\mathrm{n(r)}}{/\mathrm{r} - \mathrm{r}'/} + \mathrm{v_{xc}(r;[n])} \qquad (3.3)$$

$$\mathrm{n}(r) = \sum_i^N f_i / \varphi_i(r) \; /^2 \qquad (3.4)$$

Where f_i is the occupation factor of electrons ($0 \leq f_i \leq 2$). The KS equation looks like single particle Schrödinger equation, however the equation above with integration sign is the Hartree energy due to electrostatic interaction of electronic cloud and $V_{xc}(r; [n])$ is exchange-correlation potential, reminiscence from Hartree-Fock theory, it includes all the remaining/unknown energy corrections) terms depend on n(r) i.e., on ψ_i which in turn depends on V_{ext}. Therefore the problem is non-linear. The $V_{ext}(r)$ can includes the potential energy due to nuclear field, and external electric and magnetic fields if present.

3.1.4 Exchange-correlation functional

The outcomes of the KS scheme indicate that achieving the minimum energy state involves constraining the energy functional and solving a set of single-particle equations. However, a major challenge in the KS scheme is accurately determining the exchange-correlation energy (E_{xc}). A precise(exact) determination of the exchange-correlation energy would provide an exact

solution to a many-body problem. At present, there is no precise solution available for this issue. Therefore, approximations such as **LDA** and **GGA** are commonly used to estimate $\mathbf{E_{xc}}$.

3.1.5 Local Density Approximation (LDA)

The energy functional is a mathematical function that depends on the local charge density at a specific point in space.

$$E_{XC}^{LDA}[n] = \int n\,(r)\varepsilon_{XC}\big(n(r)\big)dr \qquad (3.5)$$

$$v_{xc}(r) = \varepsilon_{XC}\big(n(r)\big) + \mathrm{n}(r)\frac{\mathrm{d}\,\varepsilon_{XC}(n)}{dn} \qquad (3.6)$$

The value of $E_{xc}(n)$ is calculated for a uniform electron gas with a density of n (using Quantum Monte Carlo methods) and then adjusted to fit an analytical expression.

3.1.6 Generalized Gradient Approximation (GGA)

This category comprises functionals that rely on both the local density and the local density gradient :

$$E_{xc} = \int n(r)E_{GGA}\,(n(r),|\,\nabla n(r)|)dr \qquad (3.7)$$

There are various types of functionals available for this purpose, including advanced options such as Meta-GGA (e.g., SCAN), hybrids (e.g., B3LYP), and nonlocal functionals designed for van der Waals forces, such as Grimme's DFT+D (a semi-empirical correction to GGA). While these functionals typically yield more precise outcomes, they can be computationally intensive and occasionally prone to numerical instability.

3.2 Pseudopotentials and Applications

The pseudopotential concept, also referred to as the standard model for condensed phases, has greatly enhanced our comprehension of semiconductor electrical structure. This section delves into the ab-initio and empirical pseudopotentials, along with their diverse uses. Empirical pseudopotentials were first employed to explain the optical and dielectric characteristics of

tetrahedral semiconductors, and it was subsequently demonstrated that the resultant depiction of a one-electron band structure was accurate. Despite being created more than three decades ago, the band structures continue to be highly precise. Recent approaches to comprehending the chemical bonding in solids involve the integration of density functional theory and pseudopotentials. These methods have been successful in accurately forecasting the compressibility, vibration patterns, phase stability, and structural characteristics of semiconductors in different conditions. (Stewart Clark, 2012) The idea of pseudopotentials revolves around the separation of valence and core electrons in terms of energy and space. These pseudopotentials are commonly adjusted using Gaussian functions to be utilized in regular quantum espresso computational software. Various methods exist for developing pseudopotentials in the context of density functional theory (DFT). These methods include utilizing parameterized analytical pseudopotentials and generating pseudo potentials using pseudo orbitals obtained from atomic calculations. The discrete variation method (DVM), a specific approach to numerical integration for solving the DFT one electron equations, eliminates the need to fit pseudo orbitals to analytical functions. Instead, the matrix elements of an effective Hamiltonian can be directly calculated using either analytical or numerical basis sets, or a combination of both. (Stewart Clark, 2012).

One benefit of using a plane wave basis is the convenience in adjusting its precision (accuracy), however, a notable drawback is that the size of the necessary basis set for a specific system is typically larger compared to a localized basis set. This is due to the fact that in condensed matter systems, orbitals tend to exhibit smoother fluctuations in certain areas and rapid oscillations near atomic nuclei. To accurately represent these rapid oscillations, a high cut-off energy is required to incorporate plane waves with short wavelengths. Nevertheless, a large portion of the computational expenses associated with these plane waves are inefficiently utilized as most of the space within the cells does not contain rapidly oscillating orbitals. Utilizing pseudopotentials in combination with plane waves offers a solution to the challenge at hand. By substituting the

highly fluctuating core electrons with a more uniform potential, calculations of the electronic structure of a system can be carried out more effectively. To understand what Pseudopotentials does we note the following facts about orbitals in condensed matter system:

1. Core electrons are electrons found in lower energy orbitals that are strongly attracted to the nucleus of an atom. These electrons are typically unaffected by the atom's surrounding chemical conditions and are highly concentrated near the nucleus.
2. The non-core electrons orbiting near atomic nuclei exhibit rapid oscillations, however, many of these oscillations can be ignored as they are required to be perpendicular (orthogonal) to the core electrons. Therefore, the orbitals of non-core electrons need to be designed differently from the core electrons' orbitals to suppress specific oscillations.

Pseudopotential theory involves the introduction of a hypothetical potential to substitute the core electrons, maintaining the unchanged behavior of valence electrons at a distance from the nucleus, effectively representing the nuclear charge. The interactions between atoms influence the properties of condensed matter, and the pseudopotential approximation should not drastically change these properties as long as it does not interfere with regions involved in chemical bonding. Utilizing pseudopotentials helps decrease the computational expenses of calculations in three ways:

1. By excluding core electrons from the calculations, the number of Kohn-Sham orbitals is reduced. This decrease helps in lowering the memory requirements for storing the orbitals and reduces the time needed for orthogonalizing a set of orbitals.
2. When core electrons are not present to cause interference, valence electrons can align themselves more efficiently, resulting in less disturbance to the orbitals near the nucleus. As a result, orbitals can be represented with a lower energy threshold, which speeds up calculations and reduces memory usage. This decrease in energy threshold can greatly improve efficiency, often leading to significant advancements in computational speed.

3. The form of the pseudopotential is changeable rather than fixed for a specific element, allowing for optimization to reach the lowest feasible cut-off energy. This optimization leads to faster processing and lower memory utilization, which contributes to greater computational efficiency.

3.2.1 Ultra Soft Pseudopotentials (USPP)

In order to reduce the required basis set size even further, ultrasoft pseudopotentials relax the norm-conserving condition, which, however, leads to the creation of a generalized eigenvalue problem. (Vanderbilt David, April 1990).

3.2.2 Quantum Espresso (QE)

Quantum ESPRESSO is a free set of quantum chemistry techniques for materials modeling and electronic structure simulations, distributed under the GNU General Public License. It is based on density functional theory, plane wave basis sets, and norm-conserving and ultrasoft pseudopotentials. The package, known as ESPRESSO, is an open-source initiative led by the CNR-IOM DEMOCRITOS National Simulation Center in Trieste, Italy, in collaboration with other global research centers including MIT, Princeton University, the University of Minnesota, and the Ecole Polytechnique Federale Lausanne. (Paolo Giannozzi et al., 2009)

The package is made up of a set of core programs, largely written in Fortran-90 but with some pieces in C or Fortran 77, that perform critical plane wave DFT operations. These fundamental programs include Car-Parrinello molecular dynamics (CP), data analysis and charting (Post Proc), and solving the self-consistent Kohn and Sham equations in a periodic solid (pwsef). Additional packages include Phonon, which computes second and third order derivatives of energy with respect to atomic displacement using Density-Functional Perturbation Theory, Atomic, which generates pseudopotentials, and NEB, which calculates reaction paths and energy barriers.

The Open-Source Package for Research in Electronic Structure, Simulation, and Optimization (ESPRESSO) was originally released as a separate project, but its Plane-Self-Consistent Field (PWSCF) component is now the cornerstone of Quantum ESPRESSO. The package was initially

made accessible on June 15, 2001, and has since been continuously expanded and improved by the project's global collaboration of research centers and organizations.

&CONTROL

```
 calculation = ‘scf’,
 prefix= ‘PbTe’
 pseudo_dir = ‘/home/ben/PSEUDOPOTENTIALS/' ,
 outdir = ‘./’,
/
```

&SYSTEM

```
 Ibrav=2,
 celldm(1)=12.4400,
 nat=2, ntyp=2, occupations= ‘smearing’, smearing= ‘mv’, degauss=0.01
 ecutwfc=75,
/
```

& ELECTRONS

```
 mixing_beta = 0.7
 conv_thr =1.0d-8
```

ATOMIC_SPECIES

```
Pb     207.20000        Pb_pbe-dn-kjpaw_psl.0.2.2.UPF
Te      127.60000        Te_pbe-dn-kjpaw_psl.0.3.1.UPF
```

ATOMIC_POSITIONS {crystal}

Pb 0.00000000 0.00000000 0.00000000

Te 0.50000000 0.50000000 0.50000000

K_POINTS (automatic)

8 8 8 0 0 0

3.2.3 Post Processing

Stefano Baroni, Stefano de Gironcoli, Andrea Dal Corso (from SISSA), and Paolo Giannozzi (from the University of Udine) developed the post-processing calculation program, together with several additional collaborators. (www.quantum-espresso.org) Following the self-consistent calculation, we perform smaller computations such as visualizing bands and computing the density of states (DOS). The key post-processing algorithms that extract the needed data/files from the PWSCF calculations and execute subsequent calculations are as follows:

1. **P.W.X:** We use this command to run input files of scf and nscf calculations of energy and wave functions at each and every k-points, which extracts the output files for the energy calculation at every k-points.
2. **Bands.x:** To prepare the data for processing, this extracts the files from the PWSCF computations and logs the eigenvalues at various k-points, along with the related energy values. The code bands are also used to do symmetry analysis on the band structure.x.
3. **Plotband.x:** The auxiliary codes for plotband.x are designed to process output files from bands.x and convert them into a format suitable for plotting. It is important to ensure that the k-points are arranged in the correct order to avoid unexpected results in the plots. Proper sequencing of the k-points is essential to generate accurate plots.

4. **Dos.x:** This code helps us to calculate the electronic density of states at different k-points.
5. **Thermo_pw.x:** This Fortran driver utilizes Quantum ESPRESSO (QE) routines as the primary engine for efficiently calculating material properties in a parallel and/or automatic manner. It produces postscript figures depicting various material properties by utilizing the same input as the QE PW.x code. (github.io)

3.2.4 Band Structure

The electronic band structure is a popular analytical technique for calculating the first-principles electronic structure of crystals, notably within the Kohn-Sham density functional theory framework. It defines the electronic levels in (perfect) crystal formations using a band index (n) and a Bloch vector (K). The Bloch vector is a reciprocal space element measured in length units that is normally limited to the first Brillouin Zone. (Andreas Wacker, 2010). A solid's band structure, which serves as the foundation for the majority of crystal characteristics, can be utilized to determine a variety of electrical properties. When a large number of atoms come together, their interaction disrupts the initial atomic levels due to the close packing of atoms in a solid. Pauli's Exclusion Principle states that no two electrons may occupy the same energy state, implying that all of the electrons in the orbitals are full up.

Interatomic interactions have the least effect on electrons in a band's inner shell, whereas electrons in the valence band, which are closest to neighboring ions, have the greatest impact. This results in the formation of an energy continuum in which separate levels created by individual atoms cannot be distinguished. When an atom comes into contact with another, a single, sharp level splits. The band structure of a material can be utilized to determine its many optical and electrical features. Band theory states that the measurement of the band gap determines the type of solid. In density functional theory (DFT), band structures are calculated

using the pseudopotential and plane wave basis set approaches. The exchange correlation functional is treated with the Generalized Gradient Approximation (GGA) in the form of the Predew Berke-Erzndof (PBE) function.

3.2.5 Density of State (DOS)

The term "Density of States" (DOS) refers to the number of states that particles can occupy in a particular energy range per unit energy (Walter, 1989). In other words, it is a measure of a system's quantum state concentration, denoted by the number of quantum states per energy range unit. The density of states plays an important role in solid state and condensed matter physics because it may be used to estimate several parameters that provide insights into numerous electronic, magnetic, and transport phenomena.

3.3 Computational Details

3.3.1 Convergence Test (Optimization)

The self-consistent field (SCF) calculations were performed to ascertain fundamental parameters, specifically:

The kinetic energy cut-off for the k-points grid and plane wave basis, and

The lattice parameters, which were obtained through energy minimization.

These parameters were evaluated by examining the convergence of the total energy with respect to each of these parameters individually.

Kinetic Energy Cut-Off (Ecutwfc)

The kinetic energy cut-off (ecutwfc) determines the dimension of the plane-wave (PW) basis sets used to expand the wave function (Kohn-Sham orbitals). It is measured in Ry. In a periodic system, the amount of the kinetic energy cut-off is proportional to the proximity of the interactions. Long-range interactions can be accommodated by increasing the cut-off energy, resulting in a more exact output. However, this comes at the cost of more computational power. Although the calculations are reasonably affordable, choosing a modest energy cut-off may produce inaccurate results. Therefore, it is critical to establish the best cut-off energy value.

Procedures:

1. Change the value of ecutwfcin, scf.in(e.g si.scf.in), input file to 10,15,20,25,30,35,40,.....
2. Run pw.x again and again, noting the final energy.
3. Grep to edit the energies.
4. Complete the data in file si.etot_vs_ecut.
5. Plot file si_etot_vs_ecut

For instance

$ gnuplot (then press enter)

Gnuplot>plot 'si_etot_vs_ecut' using 1:2 with lines.

Cell Dimension (Lattice Parameter)

The lattice constant is a property of the crystal lattice, or the regular arrangement of atoms in three dimensions, regardless of whether it is an atomic property or not. Typically measured in angstroms (Å), the value for most crystals is a few angstroms. The lattice constant represents the length of the lattice's repeat unit.

Procedures:

1. Edit the celldm in the &SYSTEM structure.
2. Increase and decrease the value of lattice constant by adding 0.1 downward and subtracting 0.1 upward.
3. Run pw.x for values.
4. Grepcelldm.
5. VIM to filter.
6. |qe~6.4.1/bin/ev.x (press enter).
7. Lattice parameter or volume are in (au, ang) >ang.
8. Enter type of equation of state:
9. 1= birch1, 2= birch2, 3= Keane, 4= mumaghan>4.
10. Input file >celldm.
11. Output file> celldm.out.
12. **To plot graph:**

- Gnuplot (press enter)
- Gnuplot> p 'celldm' u 1:2 wl

K-Points Grid

To accurately record periodicity, a sufficiently dense grid of k-points is required. Having a large number of grid points is essential for discretely portraying interactions within the Brillouin zone. However, practical constraints on computational resources often necessitate optimizing the number of k-points grids. By calculating total energy versus k-point grids. The rectangular grid of points of dimensions k x k x k, spaced evenly throughout the Brillouin zone is called k-points grid.

Procedures:

1. Edits, scf.in(set ecutwfc back to optimized value), modifying the k-points card to use
2. K points automatic, nk1 nk2 nk3.

3. Run pw.x complete entries for each k points.
4. Grep.
5. VIM to filter.
6. Plot the graph using the following syntax:

   $gnuplot...press enter

   Gnuplot> plot 'si.etot_vs_nks' using 1:2 wl

3.3.2 Band Structure

Procedures:

1. Open a new folder and name it 'Band'
2. Copy the following files into the folder and edit all

   scf.in

   nscf.in

   band.in

3. Open terminal/cd…

   cd/element/Band

start with scf.in

   nscf.in

   band.in

Code to compute band structure calculation

$~/qe-6.4.1/bin/pw.x<scf.in>scf.out

$~/qe-6.4.1/bin/pw.x<nscf.in>nscf.out

$~/qe-6.4.1/bin/pw.x<band.in>band.out

To plot graph:

$~/qe-6.4.1/bin/plotband.x(press return)

Input file:>ba.bands.dat(press enter)

Range:-0.000 413.150ev Emin Emax 0.0, 413 (press enter)

Output file (xmgr) > ba.xmgr (press enter)

Output file(ps)>ba.ps(press enter)

Fermi>0.00 (press enter)

Delta Fe, reference E (for ties) 50,0

3.3.3 Density of States (Dos)

How to calculate for DOS:

1. Open a new folder, name it 'DOS'
2. Copy the following files into the folder and edit

   scf.in

   nscf.in

   dos.in

   pdos.in

note: all files were edited with respect to material name and scf.in

3. Open terminal/cd..

Cd[space]/element/Dos

Start with

a) scf.in pw.x<PbTe.scf.in>PbTe.scf.out

b) scf.in pw.x<PbTe.nscf.in>PbTe.nscf.out

c) dos.in dos.x<PbTe.dos.in>PbTe.dos.out

d) pdos projwfc.x<PbTe.pdos.in>PbTe.pdos.out

3.4 Post Processing

The package called post processing was originally developed by Stefano Baroni, Stefano de Gironcoli, Andrea Dal Corso, and many others. After the self-consistent calculation has been converged. They are number of auxiliary codes performing small calculations such as plotting of band, density of state (DOS) etc. The main post processing codes which extract the specified data/files from PWscf calculations and perform further calculations are as follows:

pw.x: we use this command to run the input files of scf and nscf calculations of energy and wave functions at each and every k-points, which extracts the output files for the energy at every k-points. Also it is used to calculate electronic structure, structural optimization, molecular dynamics

ph.x: This command is used to calculate the phonon frequencies and displacement patterns, dielectric tensors, effective charges (using data produced by pw.x)

q2r.x: This code calculates the Interatomic Force Constants(IFC) in real space from dynamical matrices produced by ph.x on a regular q-grid.

matdyn.x: This codes helps in producing phonon frequencies at a generic wave vector using the IFC file calculated by q2r.x; which may also calculate phonon DOS.

pp.x: This extracts the specified data form files produced by pw.x, prepared data for plotting by writing them into formats that can be read by several plotting programs.

bands.x: This extracts the files from PWscf calculation and records its eigenvalues at different k-points with corresponding energies values ready for further processing. The code bands.x also performs the symmetry analysis of the band structure.

plotband.x: This codes reads the output files of bands.x, and then produces band structure for Post Script plots.

dos.x: This command is used to calculate the electronic Density of State (DOS) at different k-points.

Projwfc.x: This code helps in calculating the projections of wave function over atomic orbitals s,p,d,f

CHAPTER FOUR

RESULTS AND DISCUSSION

4.1 Discussion of Results

4.1.1 Structural and Mechanical Properties

PbTe crystallizes in a face-centered cubic (FCC) structure, with each Pb and Te atom creating a rock salt (NaCl) lattice.

To investigate the structural properties of the PbTe perovskite compound, firstly the structural optimization was carried out by minimizing the total energy of the compound concerning modifications in the lattice parameters.

This optimization allowed for a thorough analysis of the structural properties associated with the ground state configuration of the PbTe perovskite. The crystal structure of PbTe is presented in figure 4.1 below.

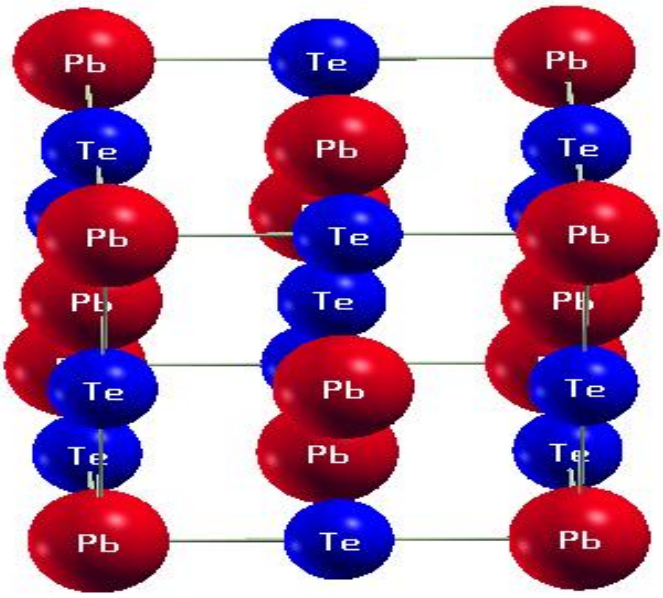

Figure 4.1: Crystallographic structure of PbTe Perovskite compound.

Table 4.1 shows the lattice parameters, a (Å), which represent the spacing between neighboring atoms, and the bulk modulus, B (GPa).

Table 4.1: Factors that contribute to the structural properties of the PbTe Perovskite material

S/N	Perovskite compound	PbTe
i	a (Å)	6.5824
ii	B(Gpa)	35.71

The numbers in Table 4.1 were determined from a sequence of self-consistent computations (SCF) performed during the optimization process described in Chapter 3. The bulk modulus indicates a material's resistance to compression, whereas the pressure derivative evaluates its responsiveness to small pressure fluctuations.

Deformation resistance refers to a material's capacity to tolerate compressive forces. Mechanical parameters that quantify this resistance include the Bulk Modulus (B, measured in GPa), Young Modulus (E, also measured in GPa), Shear Modulus (G, also measured in GPa), elastic constants (C11, C12, C44), and caunchy pressure (Cp = C12 - C44). These parameters are presented in Table 4.2.

Table 4.2: Factors that contribute to the mechanical properties PbTe Perovskite compound

S/N	Mechanical Property	PbTe
I	E (GPa)	57.61
Ii	G (GPa)	23.51
Iii	B/G	1.519
Iv	N	0.22527
V	C_{11} (GPa)	98.4
Vi	C_{12} (GPa)	4.4
Vii	C_{44} (GPa)	14.2
Viii	C_{12} (GPa) - C_{44} (GPa)	-9.8
Ix	C_{11} (GPa) + $2C_{12}$ (GPa)	107.2

The Poisson ratio and elastic constants are computed to ensure the compound's mechanical stability against shear stress. The Poisson ratio of a perovskite material offers information about its elasticity and deformation properties; a positive Poisson ratio indicates steady tensile deformation, whereas a negative Poisson ratio indicates compressive deformation. The Poisson ratio of PbTe indicates that it has steady tensile deformation.

Elastic constants, along with other structural properties, are critical for determining solid material stability (Wu Z., 2007). In cubic phases, stability is evaluated using the criteria stated in equations (4.1), (4.2), and (4.3) (Smirnow N.A., 2002).

$C_{11} > 0$ (4.1)

$C_{44} > 0$ (4.2)

$C_{11} + 2C_{12} > 0$ (4.3)

Table 4.2 displays the elastic constant data required for these equations, and the results reveal that PbTe meets the necessary conditions, indicating that it is stable.

The Cauchy pressure can be used to describe the type of bonding in a material. A negative Cauchy pressure indicates a strong resistance to bond bending, which is characteristic of covalently bonded materials. Metallically bonded materials, on the other hand, exhibit positive Cauchy pressure. This attribute is important for understanding materials' mechanical behavior and response to external pressures. Equation (4.4) shows how to compute this pressure using the cubic material's crystal elastic constants. The Cauchy pressure of -9.8, as shown in Table 4.2, suggests that the material is covalent.

$$C_p = C_{12} - C_{44} \quad (4.4)$$

Pugh's ratio is also used to determine the material's ductile or brittle nature. Pugh identified a correlation between a compound's ductility or brittleness and the Bulk Modulus to Shear Modulus ratio in 1954 (S. F. Pugh, 1954). A critical value of 1.75 for the B/G ratio is considered significant: B/G > 1.75 suggests ductility, while B/G < 1.75 indicates brittleness (pubs.rsc.org). This ratio serves as a valuable indicator of a material's mechanical properties and its tendency to deform plastically or fracture under stress. PbTe Perovskite compound has a Pugh's ratio of 1.519, hence it is a brittle material in nature.

4.1.2 Electronic and Magnetic Properties

Figures 4.2, 4.3, and 4.4 below show the electronic band structures and density of states of the PbTe perovskite material as determined by the ab initio computation of its electronic characteristics. The PbTe exhibits semiconductor characteristics due to a narrow band gap between the valence and conduction bands in both its upward and downward spin.

The calculations of electronic band structure of PbTe have been carried out by using k.p perturbation theory. The band gap of PbTe was obtained to be 0.98eV by SCF calculations. PbTe's narrow band gap makes it suitable for infrared optoelectronic devices. Additionally, it was found to be suitable for photoconductive applications. It possesses several special characteristics, such as a large refractive index, a negative pressure coefficient, a positive temperature coefficient, and smaller Auger recombination rate, when compared to other semiconductors with narrow band gaps. It has a lot of potential for thermoelectric applications because of its high carrier mobility and low thermal conductivity compared to other semiconductors.

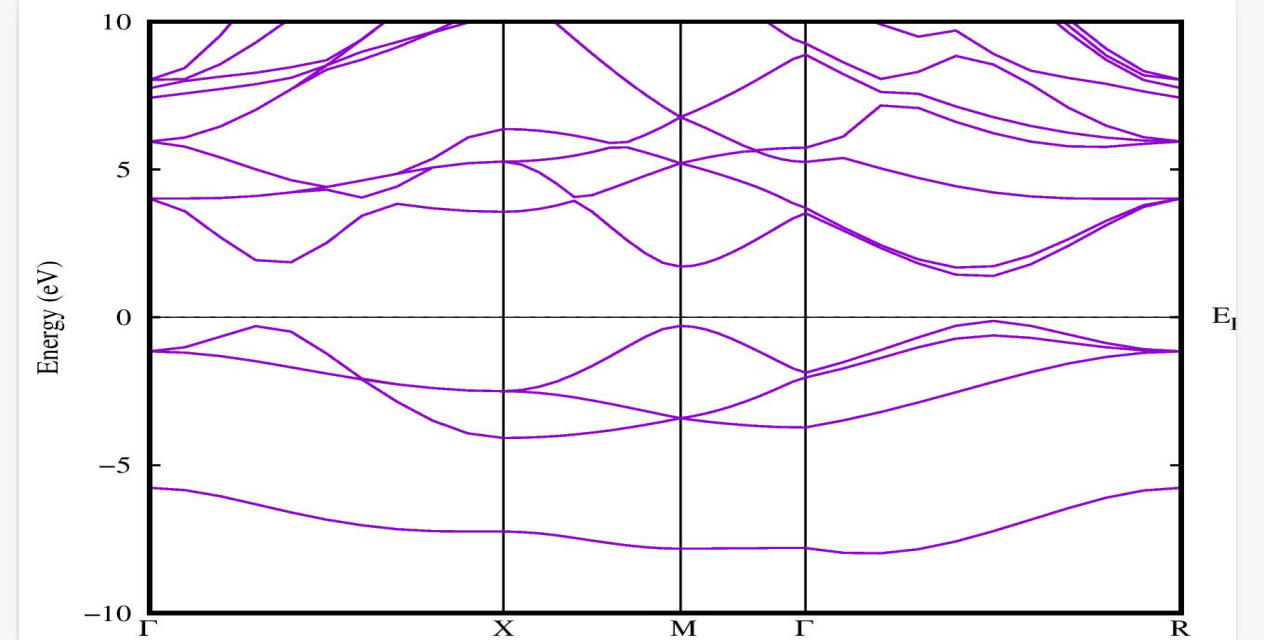

Figure 4.2: Up band spin for PbTe Perovskite compound

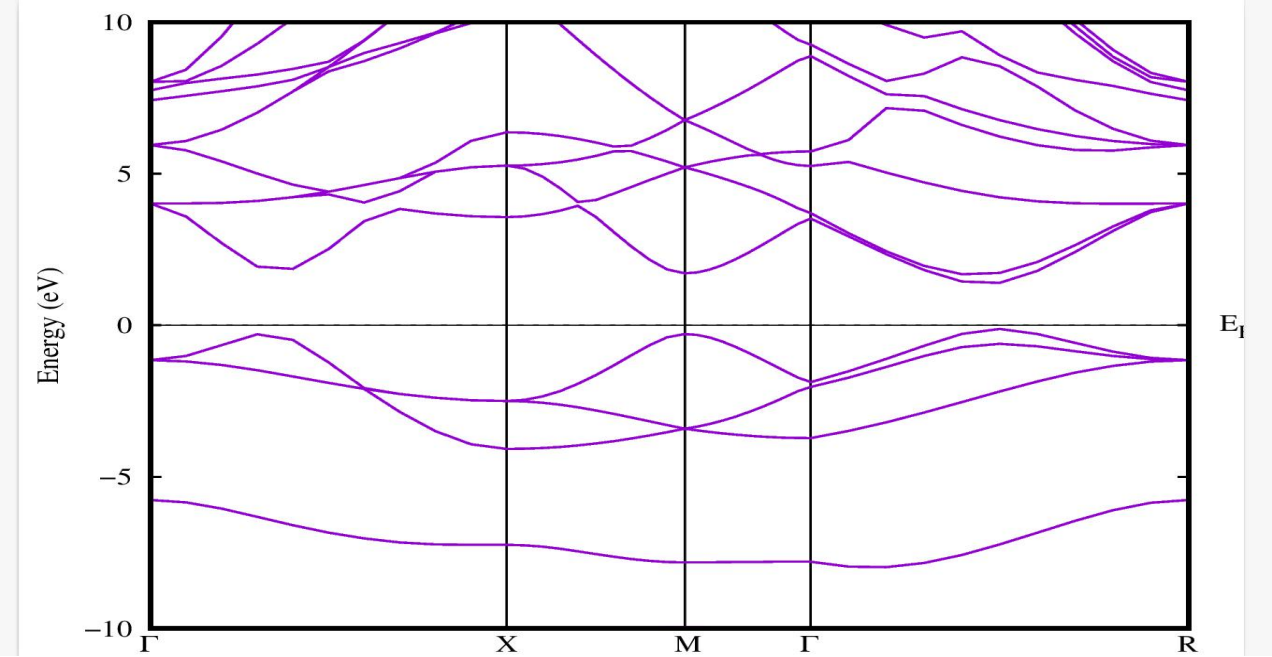

Figure 4.3: Down band spin for PbTe Perovskite compound

The PDOS plot aims to illuminate the bonding nature between orbitals and the impact of individual orbitals on the Density of States (DOS). Within the conduction band the major contribution originated from the Pb-2p orbital and the least from Te-2p orbital. Similarly in the valence band the major contribution is from Te-2p orbital and the least from Pb-2p orbital.

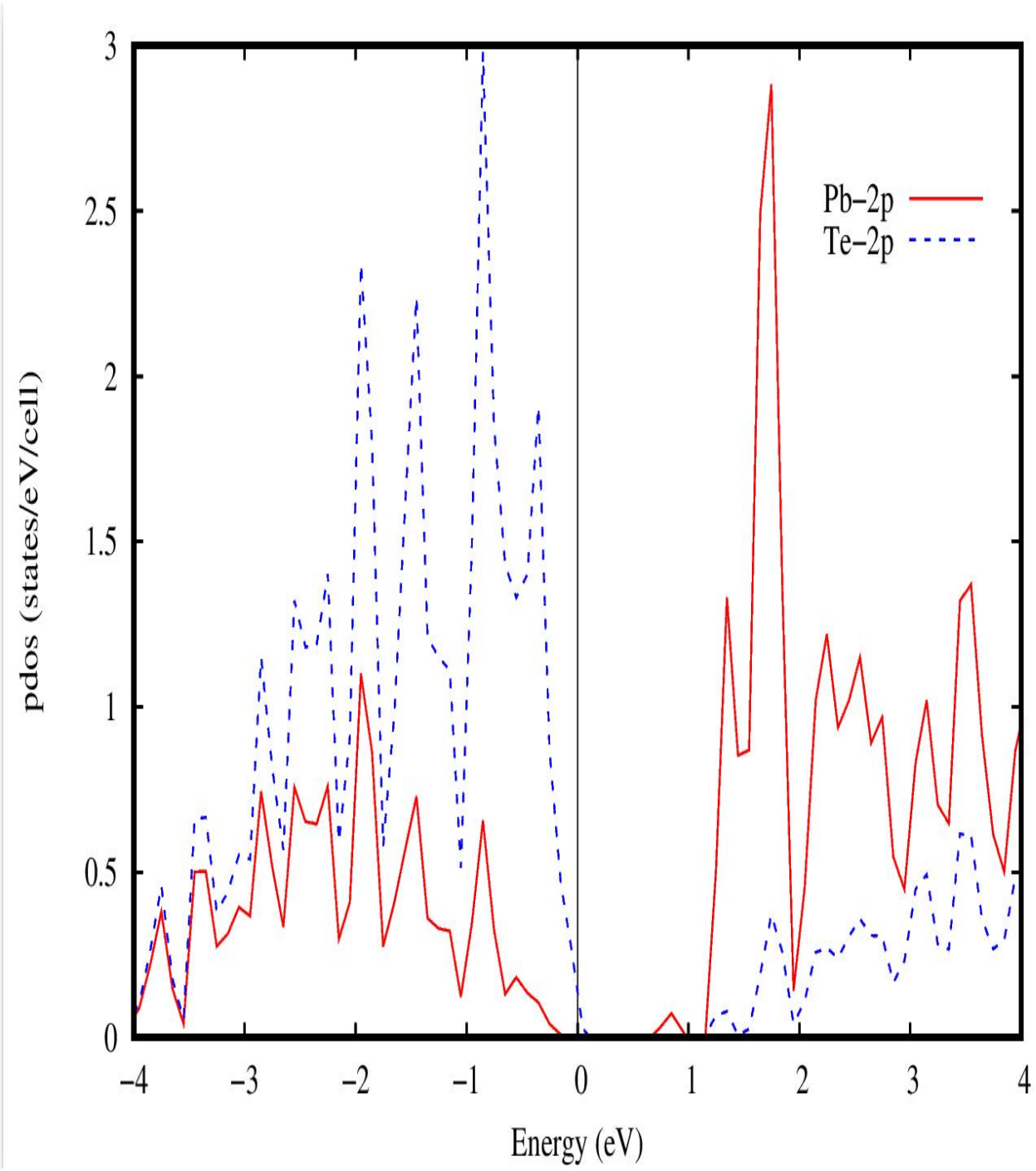

Figure 4.4: Density of state of the PbTe Perovskite compound

4.1.3 Optical Properties

The optical properties of the PbTe compound under hydrostatic pressure in the 0–9eV range are presented in Figures 4(a-h). The optical characteristics are calculated using the complex dielectric function $\varepsilon(\omega)=\varepsilon_1(\omega)+i\varepsilon_2(\omega)$, where $\varepsilon(\omega)$ represents the interaction of incoming radiation with matter. The complex dielectric function describes the linear response of a system to external electromagnetic radiation. The momentum matrix elements between the occupied and unoccupied wave functions are used to calculate the dispersion of the imaginary part of the complex dielectric function $\varepsilon_2(\omega)$, and the real part of the dielectric function $\varepsilon_1(\omega)$ is calculated using the Kramers–Kronig transformation . The real part of the dielectric constant, which is the electronic part of the static dielectric constant, is an important quantity in the zero frequency limits. The static dielectric constants is 5.72. This result is in close agreement when compared with the literature. The maximum peak in the imaginary part of the dielectric function $\varepsilon_2(\omega)$ spectra of the compound at 0GPa occur at 5.67eV.We can calculate the essential optical functions such as refractive index $n(\omega)$, absorption coefficient spectrum $\alpha(\omega)$, reflectivity $R(\omega)$, electron energy-loss spectrum $L(\omega)$, the extinction coefficient $k(\omega)$ and optical conductivity by understanding the real and imaginary parts of the dielectricfunction. The absorption coefficient is a key component since it informs us about the best solar energy conversion efficiency and reveals how much light of a specific energy or frequency may pass through a material before it is absorbed. The absorption coefficient describes the intensity attenuation of the light passing through a material. It can be understood as the sum of the absorption cross-sections per unit volume of a material for an optical process. For 0GPa, the absorption coefficient increased from 1.0eV, up to 5.0eV, and then declined to some extent before increasing sharply from 5.21eV to 8.47eV. The highest peaks for 0GPa is $30(\omega)$. The PbTe seems to have a good absorption coefficient since it has a wide range of about 2eV-7eV and ocurring at low energy region. Figure

4(e) shows the computed reflectivity R(ω) of the investigated compound in the energy range of 0 to 9 eV. The reflectivity of the incident radiation attains its peak value in the far-infrared region close to 80%-90% at 6.5eV for 0GPa . The calculated refractive index n (ω) from the complex dielectric function is presented in Figure 4c. The static refractive indexes n (0) values found at zero frequency limit is 2.41 for 0GPa. The electron energy loss function, L (ω) is a critical optical characteristic that indicates the potential for rapid electron interactions inside a material. These interactions are responsible for intraband transitions, phonon excitation, inner shell ionizations, and plasmon excitations in addition to interband transitions.. In Figure 4(g), the L(ω) shows three sharp peaks, at 7.0eV, 7.86eV and 8.21eV for 0GPa. The peaks are mainly around the far infrared regions. The computed L (ω) is minimum in the infrared, visible, and lower ultraviolet regions,implying that PbTe has optical uses. As the amplitude of the energy loss function increases at higher energies, the imaginary part of the dielectric function gets smaller. The attenuation of electromagnetic waves in materials is described by the extinction coefficient k (ω). The calculated extinction coefficient k (ω) for PbTe at 0GPa is displayed in Figure 4(f). Within the visible light region, the value of k (ω) increases from 0.0 – 0.4 with energy and reached a maximum value of 2.4 at 6.5eV in the far infrared region. The value of k (ω) starts decaying and inactive in the high energy region.

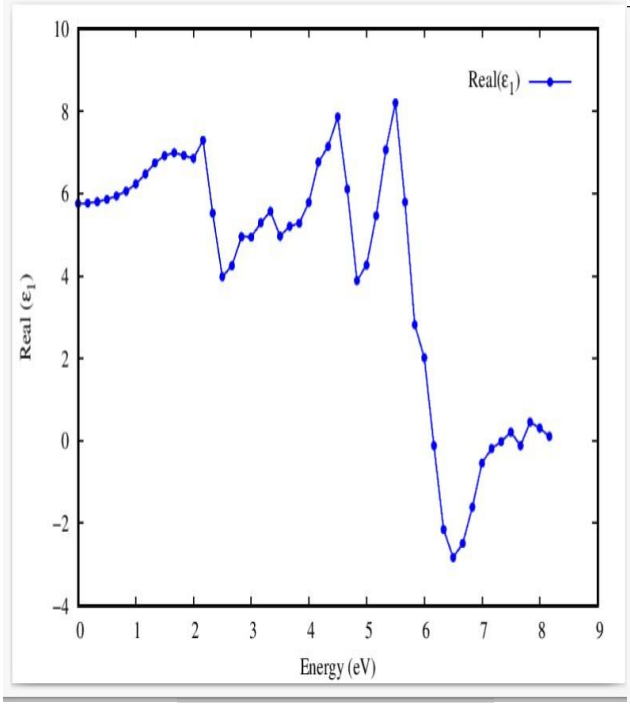

Figure 4(a)

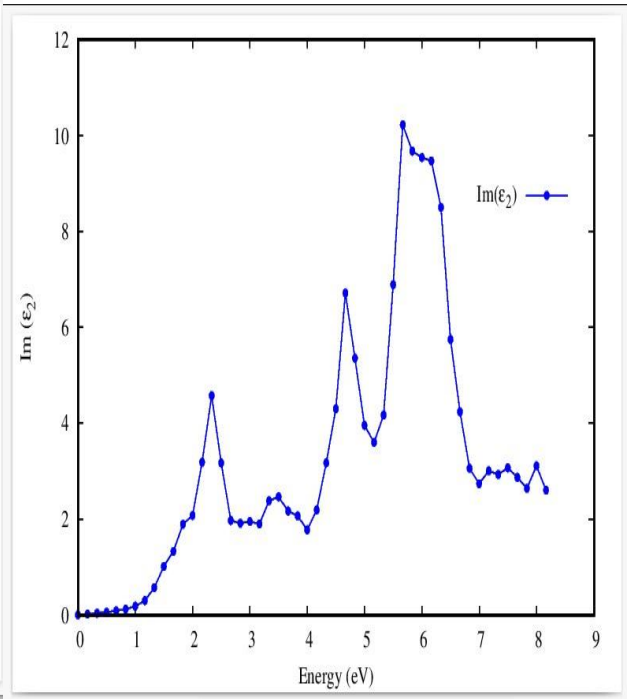

Figure 4(b)

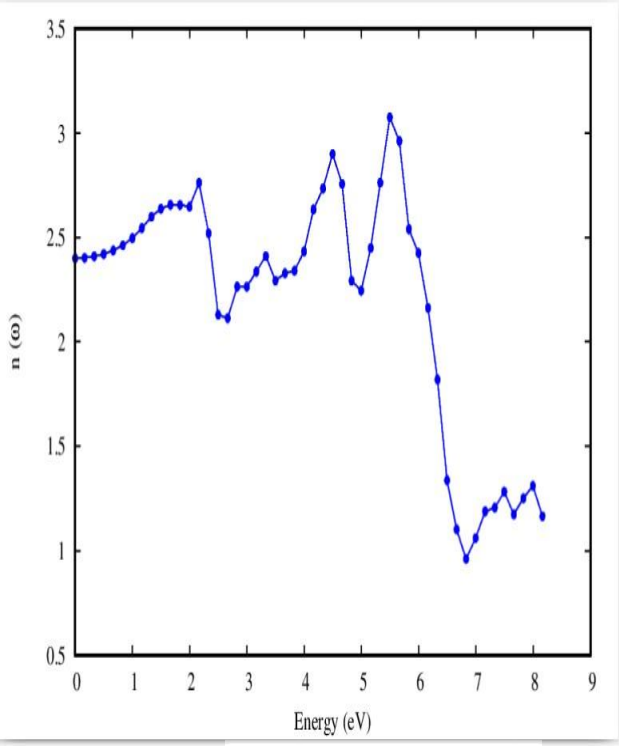

Figure 4(c)

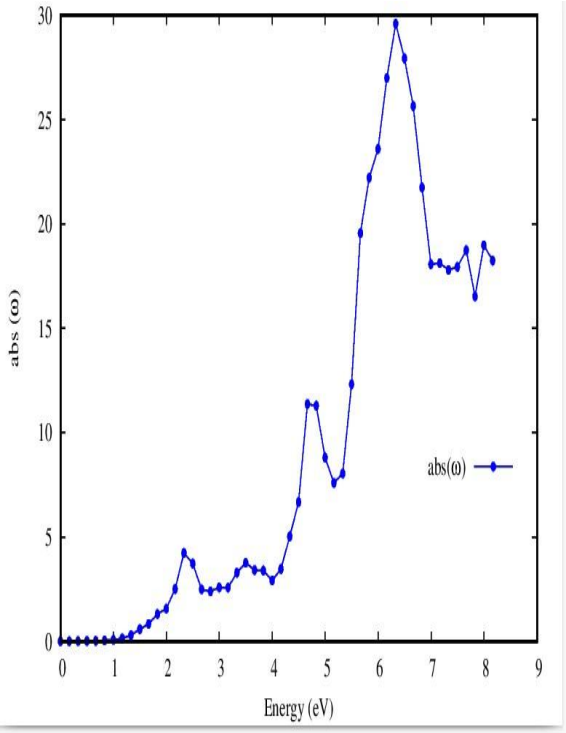

Figure 4(d)

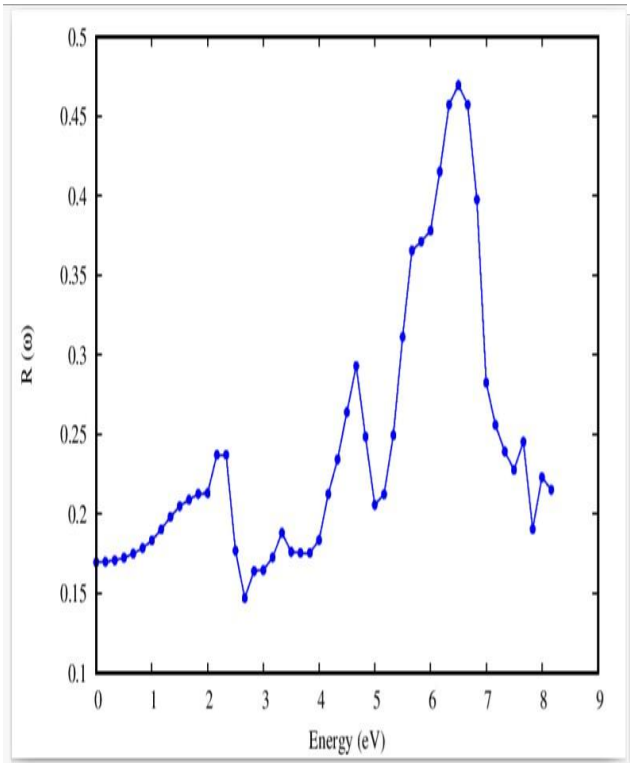

Figure 4(e)

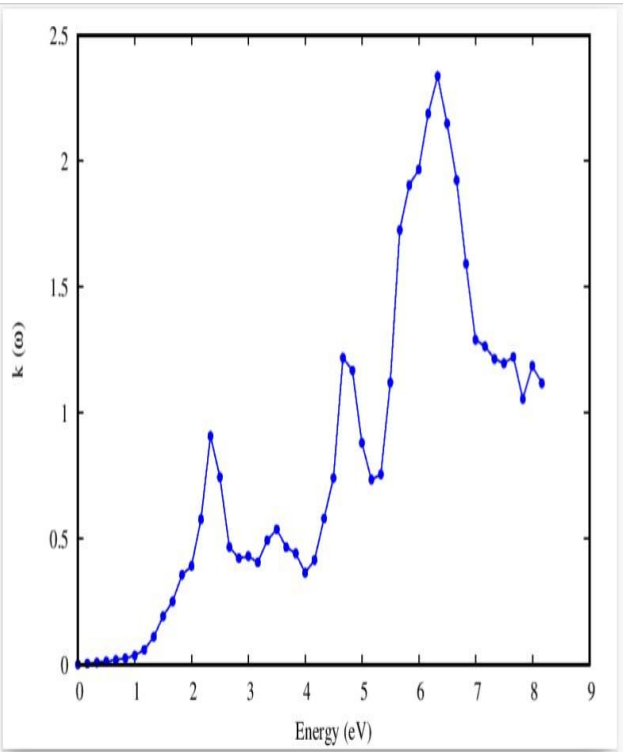

Figure 4(f)

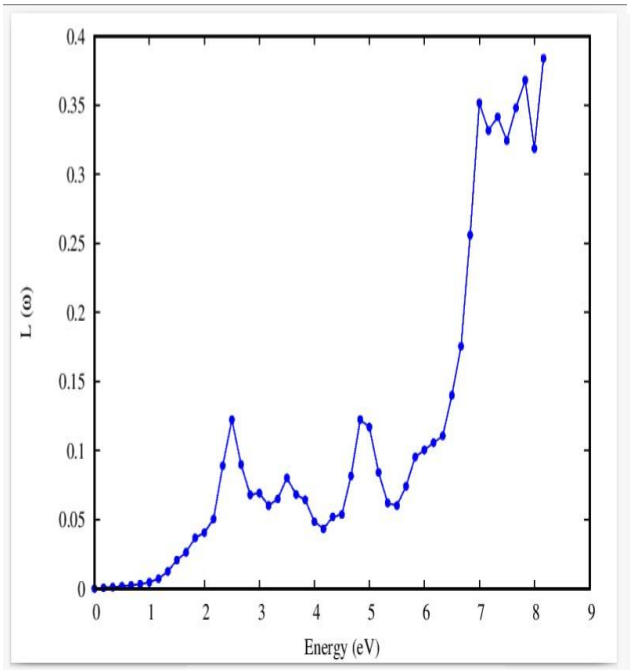

Figure 4(g)

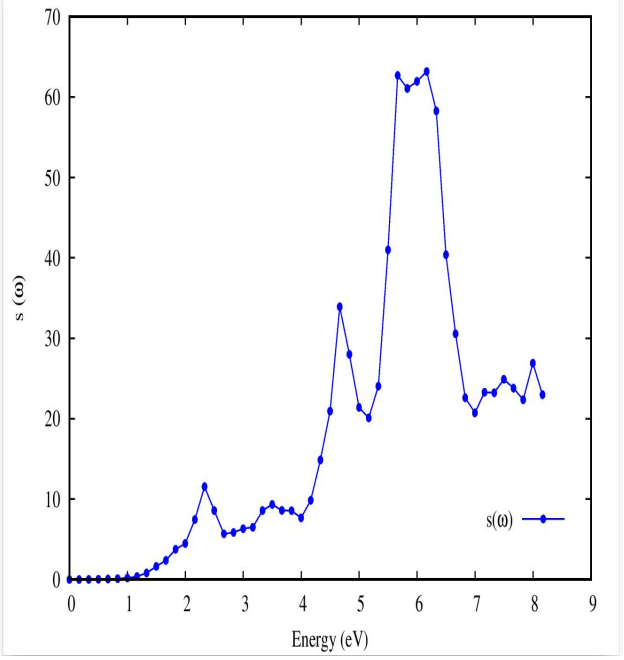

Figure 4(h)

Figure 4(a-h): (a) Real part of the dielectric function $\varepsilon_1(\omega)$, (b) Imaginary part of the complex dielectric function $\varepsilon_2(\omega)$, (c) refractive index n(ω), (d) absorption coefficient spectrum α(ω), (e) reflectivity R(ω), (f) the extinction coefficient k (ω) (g) electron energy-loss spectrum L (ω), (h) optical conductivity s(ω).

Note; where:

$$\boldsymbol{n}(\omega)=\sqrt{\frac{1}{2}(\varepsilon_1^2+\varepsilon_2^2)^{1/2}+\varepsilon_1} \quad (1)$$

$$k(\omega)=\sqrt{\frac{1}{2}(\varepsilon_1^2+\varepsilon_2^2)^{\frac{1}{2}}-\varepsilon_1} \quad (2)$$

$$\alpha(\omega)=\sqrt{2}\omega\sqrt{(\varepsilon_1^2(\omega)+\varepsilon_2^2(\omega))^{1/2}-\varepsilon_1(\omega)} \quad (3)$$

$$\mathbf{L}(\omega)=\frac{\varepsilon_2(\omega)}{\varepsilon_1^2(\omega)+\varepsilon_2^2(\omega)} \quad (4)$$

$$R(\omega)=\frac{(n-1)^2+k^2}{(n+1)^2+k^2} \quad (5)$$

$$S(\omega)=\frac{\omega\varepsilon_2}{4\pi} \quad (6)$$

CHAPTER 5

5.1 Findings and Conclusion

The optimization, mechanical properties, electronic band structure, and density of states (DOS) of the perovskite material PbTe were examined by first principle calculations using the quantum espresso program. The computations led to the following conclusions:

The physical properties of PbTe have been studied using first principle calculation.

- From Pugh's ratio (B/G), it shows that the compound is brittle.
- From the plotted band structure graph, the perovskite compound is a semiconductor
- From the calculations, the PbTe Perovskite compound is stable.

5.2 Suggestion for Further Studies

Although this study offers important new information on the optical, mechanical, electronic, and structural properties of PbTe perovskite, more research can expand its potential applications. Some ideas for future study directions are included below:

1. **Thermoelectric Performance:** Examine electron-phonon interactions and phonon transport to increase efficiency and thermal conductivity.
2. **Surface and Interface Engineering:** Examine PbTe in possible potential photovoltaic applications, thin films, and heterojunctions.
3. **Strain and Pressure Effects:** Examine the ways that high pressure or mechanical strain alters the bandgap and mechanical stability.

REFERENCES

Aksel et al., 2011,Elena Aksel, Jennifer S. Forrester, Jacob L. Jones, Pam A. Thomas, Katharine Page, R. Matthew. Monoclinic crystal structure of polycrystalline Na0.5Bi0.5TiO3 Appl. Phys. Lett., 98 (2011)

Bai et al., 2005, F. Bai, J. Wang, M. Wutting, J.F. Li, N. Wang, A.P. Pyatakov, A.K. Zvezdin, L.E. Cross, D. Viehland. Destruction of spin cycloid in (111)c-oriented BiFeO3 thin films by epitiaxial constraint: enhanced polarization and release of latent magnetization Appl. Phys. Lett., 86 (2005).

Brockmann, 2009, T. Brockmann. Piezoelectric materials;Theory of Adaptive Fiber Composites, Springer (2009), p. 205.

Cava, 2008, Robert J. Cava. Oxide superconductors; Am. Ceram. Soc., 83 (14) (2008), pp. 5-58.

Christen and Eres, 2008, H.M. Christen, G. Eres. Recent advances in pulsed-laser deposition of complex oxides; J. Phys.: Condens. Matter, 20 (26) (2008), pp. 1-27.

Deka et al., 2014, B. Deka, S. Ravi, A. Perumal, D. Pamu. Ferromagnetism and ferroelectricity in Fe doped BaTiO3; Physica B, 448 (2014), pp. 204-206.

El-Ads et al., 2015, E.H. El-Ads, A. Galal, N.F. Atta. Electrochemistry of glucose at gold nanoparticles modified graphite/SrPdO3 electrode—towards a novel non-enzymatic glucose sensor; J. Electroanal. Chem., 749 (2015), pp. 42-52.

Garg et al., 2009, K. Garg, P. Nordblad, M. Heinonen, N. Panwar, V. Sen, F. Bondino, E. Magnano, E. Carleschi, F. Parmigiani, S. Agarwal. Study of Sb substitution for Pr in the Pr0.67 Ba0.33 MnO3 system; J. Magn. Magn. Mater., 321 (2009), pp. 305-311.

Hoefler et al., 2017, Sebastian F. Hoefler, Gregor Trimmel, Thomas Rath. Progress on lead-free metal halide perovskites for photovoltaic applications: a review; Monatshefte für Chemie – Chem. Month., 9, 148 (5) (2017), pp. 795-826.

Iyorzor B. E., Babalola M. I. and Ebuwa S.O. Investigating the Effect of Hydrostatic Pressure on the Structural, Electronic, Mechanical, Lattice Dynamics and Optical Properties of the Cubic Perovskite RbTaO3: A DFT Approach (2022).

Jia et al., 2015, F. Jia, H. Zhong, W. Zhang, X. Li, G. Wanga, J. Songa, Z. Cheng, J. Yin, L. Guo. A novel nonenzymatic ECL glucose sensor based on perovskite LaTiO3-Ag0.1 nanomaterials; Sens. Actuat. B, 212 (2015), pp. 174-182.

Jin et al., 2013, C. Jin, X. Cao, F. Lu, Z. Yang, R. Yang. Electrochemical study of Ba0.5Sr0.5Co0.8Fe0.2O3 perovskite as bifunctional catalyst in alkaline media; Int. J. Hydrogen Energy, 38 (2013), pp. 10389-10393.

Kézsmárki et al., 2011, I. Kézsmárki, N. Kida, H. Murakawa, S. Bordács, Y. Onose, Y. Tokura. Enhanced directional dichroism of terahertz light in resonance with magnetic excitations of the multiferroic Ba2 CoGe2 O7 oxide compound; Phys. Rev. Lett., 106 (2011).

Kittel, 2005, C. Kittel. Introduction to Solid State Physics (eighth ed.), John Wiley & Sons Inc. (2005), p. 675.

Klaus Capelle Brazilian journal of physics, vol 36, no. 4A. (December 2006)

Lianghao et al., 2015, Y. Lianghao, C. Yonghong, G. Qingwen, T. Dong, L. Xiaoyong, M. Guangyao, L. Bin, Layered perovskite oxide Y0.8Ca0.2BaCoFeO5+δ as a novel cathode material for intermediate-temperature solid oxide fuel cells; J. Rare Earths, 33 (5) (2015), pp. 519-523.

Lu et al., 2004, H. Lu, G. Yang, Z. Chen, S. Dai, Y. Zhou, K. Jin, B. Cheng, M. He, L. Liu, H. Guo

Mourachkine, 2004, Andrei Mourachkine. Room-Temperature Superconductivity; Cambridge International Science Publishing, Cambridge, UK (2004), p. 307

Niu et al., 2015, Guangda Niu, Xudong Guo, Liduo Wang. Review of recent progress in chemical stability of perovskite solar cells; J. Mater. Chem. A, 3 (2015), pp. 8970-8980.

Ohta and Hiramatsu, 2018, Hiromichi Ohta, Hidenori Hiramatsu. Fabrication, characterization, and modulation of functional nanolayers. Part III Nanoinformatics (2018), pp. 207-235.

Ottochian et al., 2014, A. Ottochian, G. Dezanneau, C. Gilles, P. Raiteri, C. Knight, J.D. Gale. Influence of isotropic and biaxial strain on proton conduction in Y-doped BaZrO3: a reactive molecular dynamics study; J. Mater. Chem. A, 2 (2014), pp. 3127-3133.

Paolo Giannozzietal., QUANTUM ESPRESSO: a modular and open-source software project for quantum simulations of materials (2009).

Piezoelectric field effect transistor and nanoforce sensor based on a single ZnO nanowire; Nano Lett., 6 (12) (2006), pp. 2768-2772.

Positive colossal magnetoresistance in a multilayer p–n heterostructure of Srdoped LaMnO3 and Nb-doped SrTiO3 ;Appl. Phys. Lett., 84 (2004), p. 5007.

Raghavan, 2015, V. Raghavan. Material Sciences and Engineering; PHL Learnt private Limited, Delhi, India (2015), p. 463.

Retot et al., 2008, H. Retot, A. Bessiere, A. Kahn-Harari, B. Viana. Synthesis and optical characterization of SrHfO3: Ce and SrZrO3: Ce nanoparticles; Opt. Mater., 30 (2008), pp. 1109-1114.

Roni, 2018, Peleg Roni.The Perovskite Handbook (first ed.), Metalgrass LTD (2018), p. 108.

Sayyadi-Shahraki et al., 2017, Ahmad Sayyadi-Shahraki, Ehsan Taheri-Nassaj, Hassan Sharifi, Justin Gonzales, Taras Kolodiazhnyi, Nathan Newman. Origin of dielectric loss in Ba(Co1/3Nb2/3)O3 microwave ceramics; J. Am. Ceram. Soc., 101 (4) (2017), pp. 1665-1676.

Singh et al., 2011, K. Singh, A. Maignan, C. Simon, C. Martin. FeCr2O4 and CoCr2O4 spinels: multiferroicity in the collinear magnetic state? Appl. Phys. Lett., 99 (2011).

Spaldin et al., 2010, N.A. Spaldin, S.W. Cheong, R. Ramesh. Multiferroics: past, present, and future; Phys. Today, 63 (2010), pp. 38-43.

Taylor et al., 2019, Janet Taylor, Ke Zhang, Donghai Wang. Industrial and nonfood applications; Sorghum Millets, 7 (2019), pp. 393-420.

Thirumalairajan et al., 2013, Thirumalairajan, K. Girija, V. Ganesh, D. Mangalaraj, C. Viswanathan, N. Ponpandian. Novel synthesis of LaFeO3 nanostructure dendrites: a systematic investigation of growth mechanism, properties, and biosensing for highly selective determination of neurotransmitter compounds; Cryst. Growth Des., 13 (2013), pp. 291-302.

Wang et al., 2004, Jie Wang, San-Qiang Shi, Long-Qing Chen, Yulan Li, Tong-Yi Zhang. Phase-field simulations of ferroelectric/ferroelastic polarization switching; Acta Materialia, 52 (3,9) (2004), pp. 749-764.

Wang et al., 2006, Xudong Wang, Jun Zhou, Jinhui Song, Jin Liu, Xu Ningsheng, Zhong L. Wang

Wang et al., 2008,Y. Wang, Y. Sun, J. Zhang, Z. Ci, Z. Zhang, L. Wang, New red Y 0.85 Bi0.1Eu 0.05V1− yMyO4 (M= Nb, P) phosphors for light-emitting diodes; Physica B, 403 (2008), pp. 2071-2075.

Wang et al., 2010, F. Wang, C.-H. Li, T. Zou, Y. Liu, Y. Sun. Electrically driven magnetic relaxation in multiferroic LuFe2O4; J. Phys.: Condens. Matter, 22 (2010).

Wang et al., 2012, B. Wang, S. Gu, Y. Ding, Y. Chu, Z. Zhang, X. Ba, Q. Zhang, X. Li; A novel route to prepare LaNiO3 perovskite-type oxide nanofibers by electrospinning for glucose and hydrogen peroxide sensing Analyst, 138 (1) (2012), pp. 362-367.

Xiao et al., 2011, Z. Xiao, Z. Ren, Z. Liu, X. Wei, G. Xu, Y. Liu, X. Li, G. Shen, G. Han. Single crystal nanofibers of Zr-doped new structured PbTiO3: hydrothermal synthesis, characterization and phase transformation; J. Mater. Chem., 21 (2011), pp. 3562-3564.

Xin et al., 2019, Cong Xin, Philippe Veber, Mael Guennou, Constance Toulouse, Nathalie Valle, Monica Ciomaga Hatnean, Geetha Balakrishnan, Raphael Haumont, Romuald Saint Martin, Matias Velazquez, Alain Maillard, Daniel Rytz, Michael Josse, Mario Maglione, Jens Kreisel. Single Crystal Growth of BaZrO3 from the melt at 2700 °C using optical floating zone technique and growth prospects from BaB2O4 flux at 1350 °C; Cryst. Eng. Comm., 21 (2019), p. 502.

Xu, 2011, Y. Xu. Ferroelectric Materials and Their Applications; Elsevier Publisher (2011), p. 379.

Zhang et al., 2013, Z. Zhang, S. Gu, Y. Ding, F. Zhang, J. Jin. Determination of hydrogen peroxide and glucose using a novel sensor platform based on Co0.4Fe0.6LaO3 nanoparticles; Microchim. Acta, 180 (2013), pp. 1043-1049.

Zhang et al., 2017, Yuqiao Zhang, Bin Feng, Hiroyuki Hayashi, Tetsuya Tohei, Isao Tanaka, Yuichi Ikuhara, Hiromichi Ohta. Thermoelectric phase diagram of the SrTiO3–SrNbO3 solid solution system; J. Appl. Phys., 121 (18) (2017).

Zhou et al., 2018, D. Zhou, T. Zhou, Y. Tian, X. Zhu, Y. Tu. Perovskite-Based Solar cells: materials, methods and future perspectives; J. Nanomaterials, 2018 (2018), Article 8148072 15 pages.